

# Artificial Intelligence in Ovarian Cancer Histopathology: A Systematic Review

Jack Breen<sup>†1</sup>, Katie Allen<sup>2</sup>, Kieran Zucker<sup>3</sup>, Pratik Adusumilli<sup>2,4</sup>, Andy Scarsbrook<sup>2,4</sup>, Geoff Hall<sup>3</sup>, Nicolas M. Orsi<sup>\*2</sup>, and Nishant Ravikumar<sup>\*1</sup>

<sup>1</sup>Centre for Computational Imaging and Simulation Technologies in Biomedicine (CISTIB), School of Computing, University of Leeds, UK

<sup>2</sup>Leeds Institute of Medical Research at St James's, School of Medicine, University of Leeds, UK

<sup>3</sup>Leeds Cancer Centre, St James's University Hospital, Leeds, UK

<sup>4</sup>Department of Radiology, St. James University Hospital, Leeds, UK

\*Indicates joint final authors

## Purpose

To characterise and assess the quality of published research evaluating artificial intelligence (AI) methods for ovarian cancer diagnosis or prognosis using histopathology data.

## Methods

A search of PubMed, Scopus, Web of Science, Cochrane Central Register of Controlled Trials, and WHO International Clinical Trials Registry Platform was conducted up to 19/05/2023. The inclusion criteria required that research evaluated AI on histopathology images for diagnostic or prognostic inferences in ovarian cancer, including primary tumours of the ovaries, fallopian tubes, and peritoneum. Reviews and non-English language articles were excluded. The risk of bias was assessed for every model that met the inclusion criteria using the Prediction model Risk Of Bias ASsessment Tool (PROBAST). Information about each model of interest was tabulated and summary statistics were reported. Based on the results, we provided recommendations to improve study design and reporting to reduce the risk of bias and improve the reproducibility of future research in the field. The study protocol was registered on PROSPERO (CRD42022334730). PRISMA 2020 reporting guidelines were followed.

## Results

A total of 1573 records were identified, of which 45 were eligible for inclusion. These studies reported 80 total models of interest, including 37 diagnostic models, 22 prognostic models, and 21 models with other diagnostically relevant outcomes, such as tumour segmentation and cell-type classification. Models were developed using 1-1375 slides from 1-776 ovarian cancer patients. There was a wide array of model outcomes, the most common being treatment response (11/80), malignancy status (10/80), stain quantity (9/80), histological subtype (7/80), and overall survival (6/80). Older studies used traditional machine learning (ML) models with hand-crafted features, while newer studies typically employed deep learning to automatically learn features and predict model outcome(s). All models were found to be at high or unclear risk of bias overall, with most research having a high risk of bias in the analysis and a lack of clarity regarding participants and predictors in the study. Research frequently suffered from insufficient reporting and limited validation using small sample sizes, with external validations being particularly rare.

## Conclusion

Limited research has been conducted on the application of AI to histopathology images for diagnostic or prognostic purposes in ovarian cancer, and none of the associated models have been demonstrated to be ready for real-world implementation. Recommendations are provided addressing underlying biases and flaws in study design, which should help inform higher-quality reproducible future research. Key aspects to help ensure clinical translation include more transparent and comprehensive reporting of data provenance and modelling approaches, as well as improved quantitative performance evaluation using cross-validation and external validations.

## Funding

Engineering and Physical Sciences Research Council and The Tony Bramall Charitable Trust

<sup>†</sup>Corresponding author - scjib@leeds.ac.uk.

## INTRODUCTION

Ovarian cancer is the eighth most common malignancy in women worldwide [1]. It is notoriously difficult to detect and diagnose, with ineffective screening [2] and non-specific symptoms similar to those caused by menopause [3]. Encompassing primary malignant tumours of the ovaries, fallopian tubes, and peritoneum, the disease has often started to spread within the abdomen at the time of diagnosis (FIGO [4] Stage 3). This typical late stage at diagnosis makes ovarian cancer a particularly deadly disease, with the 314,000 new cases diagnosed each year translating to 207,000 deaths per year globally [1].

Most ovarian cancers are carcinomas (cancers of epithelial origin) which predominantly fall into five histological subtypes: high-grade serous, low-grade serous, clear cell, endometrioid, and mucinous. Non-epithelial ovarian cancers are much less common and include germ cell, sex cord-stromal, and mesenchymal tumours. Ovarian cancer subtypes differ morphologically and prognostically and have varying treatment options [5]. High-grade serous carcinoma is the most common form of ovarian cancer, accounting for approximately 70% of all cases [6].

Histopathology, the examination of tissue specimens at the cellular level, is the gold standard for ovarian cancer diagnosis. Pathologists typically interpret tissue stained with haematoxylin and eosin (H&E), though interpretation can be a subjective, time-consuming process, with some tasks having a high level of inter-observer variation [7, 8, 9]. In the assessment of difficult cases, general pathologists may seek assistance from subspecialty gynaecological pathology experts, and/or use ancillary tests, such as immunohistochemistry (IHC). Referrals and ancillary testing can be essential to the accuracy of the diagnostic process but come at the cost of making it longer and more expensive. Worldwide, pathologists are in much greater demand than supply, with significant disparities in the number of pathologists between countries [10], and with better-supplied countries still unable to meet demand [11].

Traditionally, pathologists have analysed glass slides using a light microscope. However, the implementation of a digital workflow, where pathologists review scanned whole slide images (WSIs) using a computer, is becoming more common. While digital pathology uptake has likely been driven by efficiency benefits [12], it has created an opportunity for the development of automated tools to assist pathologists. These tools often aim to improve the accuracy, efficiency, objectivity, and consistency of diagnosis. Such tools could help to alleviate the global workforce shortage of pathologists, increasing diagnostic throughput and reducing the demand for referrals and ancillary tests. This is an increasingly active area of research [13] and, for some malignancies, these systems are starting to achieve clinical utility [14].

In this study, we systematically reviewed all literature in which artificial intelligence (AI) techniques (comprising both traditional machine learning (ML) and deep learning methods) were applied to digital pathology images for the diagnosis or prognosis of ovarian cancer. This included research which focused on a single diagnostic factor such as histological subtype, and studies that performed computer-aided diagnostic tasks such as tumour segmentation. The review characterises the state of the field, describing which diagnostic and prognostic tasks have been addressed, and assessing factors relevant to the clinical utility of these methods, such as the risks of bias. Despite ovarian cancer being a particularly difficult disease to detect and diagnose, and the shortage of available pathologists, AI models have not yet been implemented in clinical practice for this disease. This review aims to provide insights and recommendations based on published literature to improve the clinical utility of future research, including reducing risks of bias, improving reproducibility, and increasing generalisability.

## METHODS

### Literature Search

Searches were conducted in three research databases, PubMed, Scopus and Web of Science, and two trial registries, Cochrane Central Register of Controlled Trials (CENTRAL) and the World Health Organisation International Clinical Trial Registry Platform (WHO-ICTRP). The research databases only include journals and conference proceedings which have undergone peer review, ensuring the integrity of included research. The initial searches were performed on 25/04/2022 and were most recently repeated on 19/05/2023. The search strategy was composed of three distinct aspects -

artificial intelligence, ovarian cancer, and histopathology. For each aspect, multiple relevant terms were combined using the *OR* operator (e.g. “artificial intelligence” OR “machine learning”), and then these were combined using the *AND* operator to ensure that retrieved research met all three aspects. The widest possible set of search fields was used for each search engine except for Scopus, where restrictions were imposed to avoid searching within the citation list of each article, which is not an available field in the other search engines. The terms ‘ML’ and ‘AI’ were restricted to specific fields due to the diversity of their possible meanings. To ensure the most rigorous literature search possible, no restrictions were placed on the publication date or article type during searching.

Many AI approaches build on statistical models, such as logistic regression, which can blur the lines between disciplines. When conducting searches, a previously reported methodology was adopted [15] whereby typical AI approaches were searched by name (e.g. neural networks), and other methods were searched by whether the authors described their work as *artificial intelligence*. Full details of the search implementation for each database are provided in Appendix A. The review protocol was registered with PROSPERO before the search results were screened for inclusion (CRD42022334730).

### Literature Selection

One researcher (JB) manually removed duplicate papers with the assistance of the referencing software *EndNote X9*. Two researchers (JB, KA) then independently screened articles for inclusion in two stages, the first based on title and abstract, the second based on full text. Disagreements were discussed and arbitrated by a third researcher (NR or NMO). Trials in WHO-ICTRP do not have associated abstracts, so for these studies, only titles were available for initial screening.

The inclusion criteria required that research evaluated the use of at least one AI approach to make diagnostic or prognostic inferences on human histopathology images from suspected or confirmed cases of ovarian cancer. Studies were only included where AI methods were applied directly to the digital pathology images, or to features which were automatically extracted from the images. Fundamental tasks, such as segmentation and cell counting, were included as these could be used by pathologists for computer-aided diagnosis. Only conventional light microscopy images were considered, with other imaging modalities, such as fluorescence and hyperspectral imaging, excluded. Publications which did not include primary research were excluded (such as review papers). Non-English language articles and research where a full version of the manuscript was not accessible were excluded.

A model in an included study was considered to be a *model of interest* if it met the same inclusion criteria. Where multiple models were compared against the same outcome, the model of interest was taken to be the newly proposed model, with the best performing model during validation taken if this was unclear. If multiple model outcomes were assessed in the same study, a model of interest was taken for each model outcome, regardless of any similarity in modelling approaches. The same model outcome at different levels of precision (e.g. patch-level, slide-level, patient-level) were not considered to be different model outcomes. Models didn’t need to be entirely independent, for example, the output of one model of interest could have been used as the input of another model of interest on the condition that model performance was separately evaluated for each model.

### Risk of Bias Assessment

The risk of bias was assessed for models of interest using the Prediction model Risk Of Bias ASsessment Tool (PROBAST) [16], where *risk of bias* is the chance of reported results being distorted by limitations within the study design, conduct, and analysis. It includes 20 guiding questions which are categorised into four domains (participants, predictors, outcome, and analysis), which are summarised as either high-risk or low-risk, or unclear in the case that there is insufficient information to make a comprehensive assessment and none of the available information indicates a high risk of bias. As such, an unclear risk of bias does not indicate methodological flaws, but incomplete reporting.

The **participants** domain covers the recruitment and selection of participants to ensure the study population is consistent and representative of the target population. Relevant details include the participant recruitment strategy (when and where participants were recruited), the inclusion criteria, and how many participants were recruited.

The **predictors** domain covers the consistent definition and measurement of predictors, which in this field typically refers to the generation of digital pathology images. This includes methods for fixing, staining, scanning, and digitally processing tissue before modelling.

The **outcome** domain covers the appropriate definition and consistent determination of ground-truth labels. This includes the criteria used to determine diagnosis/prognosis, the expertise of any persons determining these labels, and whether labels are determined independently of any model outputs.

The **analysis** domain covers statistical considerations in the evaluation of model performance to ensure valid and not unduly optimistic results. This includes many factors, such as the number of participants in the test set with each outcome, the validation approaches used (cross-validation, external validation, bootstrapping, etc.), the metrics used to assess performance, and methods used to overcome the effects of censoring, competing risks/confounders, and missing data. The risks caused by some of these factors are interrelated, for example, the risk of bias from using a small dataset is somewhat mitigated by cross-validation, which increases the effective size of the test set and can be used to assess variability, reducing optimism in the results. Further, the risk caused by using a small dataset depends on the type of outcome being predicted, for example, more data is required for a robust analysis of 5-class classification than binary classification. There must also be sufficient data within all relevant patient subgroups, for example, if multiple subtypes of ovarian cancer are included, there must not be a subtype that is only represented by a few patients. Due to these interrelated factors, there are no strict criteria to determine the appropriate size of a dataset, though fewer than 50 samples per class or fewer than 100 samples overall is likely to be considered high-risk, and more than 1000 samples overall is likely to be considered low-risk.

Risks of bias often arise due to inconsistent methodologies. Inconsistency in the participants and predictors domains may cause heterogeneity in the visual properties of digital pathology slides which may lead to spurious correlations, either through random chance or systematic differences between subgroups in the dataset. Varied data may be beneficial during training to improve model generalisability when using large datasets, though this must be closely controlled to avoid introducing systematic confounding. Inconsistent determination of the outcome can mean that the results of a study are unreliable due to spurious correlations in the ground truth labels, or invalid due to incorrect determination of labels.

While PROBAST provides a framework to assess risks of bias, there is some level of subjectivity in the interpretation of signalling questions. As such, each model was analysed by three independent researchers (any of JB, KA, NR, KZ, NMO), with at least one computer scientist and one clinician involved in the risk of bias assessment for each model. The PROBAST applicability of research analysis was not implemented as it is unsuitable for such a diverse array of possible research questions.

## Data Synthesis

Data extraction was performed independently by two researchers (JB, KA) using a form containing 81 fields within the categories *Overview*, *Data*, *Methods*, *Results*, and *Miscellaneous*. Several of these fields were added or clarified during data extraction with the agreement of both researchers and retroactively applied to all accepted literature. The final data extraction form is available at [www.github.com/scjjb/OvCaReview](http://www.github.com/scjjb/OvCaReview), with a summary included in Appendix B.

Information was sought from full-text articles, as well as references and supplementary materials where appropriate. Inferences were made only when both researchers were confident that this gave the correct information, with disagreements resolved through discussion. Fields which could not be confidently completed were labelled as being *unclear*.

All extracted data were summarised in two tables, one each for study-level and model-level characteristics. Only models of interest were included in these tables. The term *model outcome* refers to the model output, whether this was a clinical outcome (diagnosis/prognosis), or a diagnostically relevant outcome that could be used for computer-aided diagnosis, such as tumour segmentation. The data synthesis did not include any meta-analysis due to the diversity of included methods and model outcomes.

## RESULTS

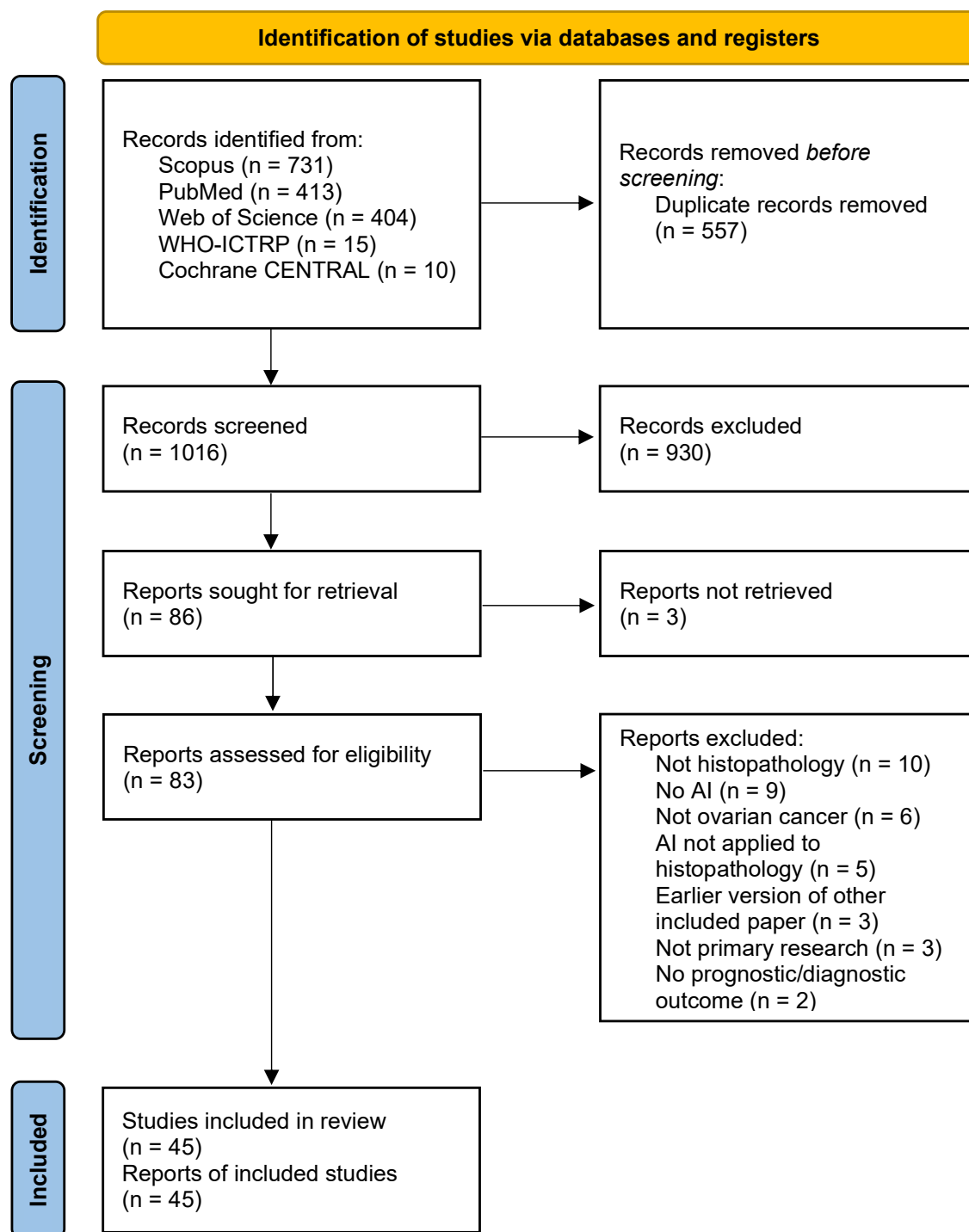


**Figure 1.** PRISMA 2020 flowchart of the study identification and selection process for the systematic review. Records were screened on titles and abstracts alone, and reports were assessed based on the full-text content. CENTRAL - Central Register of Controlled Trials. WHO-ICTRP - World Health Organisation International Clinical Trial Registry Platform.

As shown in Figure 1, the literature searches returned a total of 1573 records, of which 557 were duplicates. 930 records were excluded during the screening of titles and abstracts, and 41

were excluded based on full paper screening, including 3 records for which full articles could not be obtained. The remaining 45 studies were included in the review, of which 11 were conference papers and 34 were journal papers. All accepted studies were originally identified through searches of research databases, with no records from trial registries meeting the inclusion criteria. While the searches returned literature from as early as 1949, all of the research which met the inclusion criteria was published since 2010, with over 70% of the included literature published since 2020. Study characteristics are shown in Table 2. The 45 accepted articles contained 80 models of interest, details of which are shown in Table 3.

### Risk of Bias Assessment

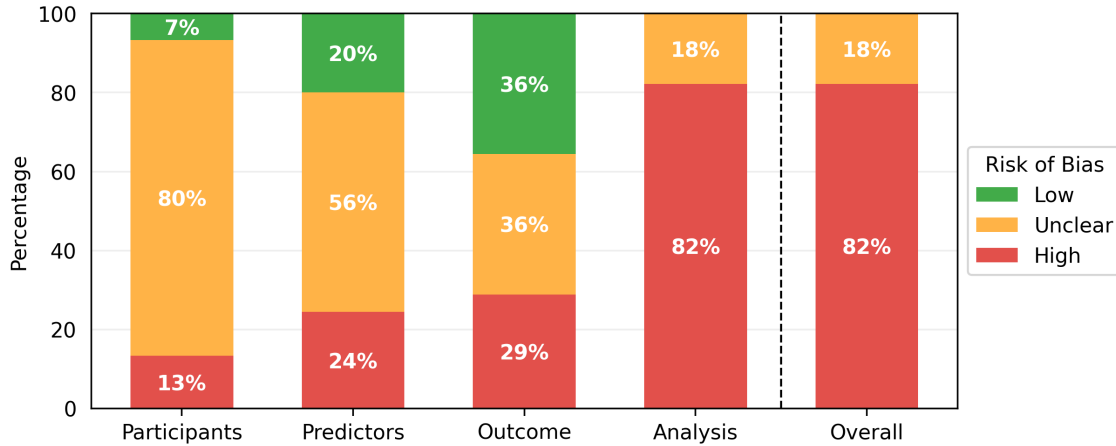


**Figure 2.** PROBABST risk of bias results summarised for the 45 papers included in this review.

The results of the PROBABST assessments are shown in Table 1. While some studies contained multiple models of interest, none of these contained models with different risk of bias scores for any section of the PROBABST assessment, so one risk of bias analysis is presented per paper. All models showed either a high overall risk of bias (37/45) or an unclear overall risk of bias (8/45). Every high-risk model had a high-risk score in the analysis section (37/45), with several also being at high risk for participants (6/45), predictors (11/45), or outcomes (13/45). Less than half of the studies achieved a low risk of bias in any domain (21/45), with most low risks being found in the outcomes (16/45) and predictors (9/45) sections. Nearly all of the papers had an unclear risk of bias in at least one domain, most commonly the participants (36/45) and predictors (25/45) domains. Qualitative summaries are presented in Figure 2.

Publication	Participants	Predictors	Outcome	Analysis	Overall
Dong 2010(a) [17]	High	High	High	High	High
Dong 2010(b) [18]	High	High	High	High	High
Signolle 2010 [19]	Unclear	Unclear	High	High	High
Janowczyk 2011 [20]	Unclear	Unclear	Low	High	High
Janowczyk 2012 [21]	Unclear	High	Unclear	High	High
Kothari 2012 [22]	Unclear	Low	Low	Unclear	Unclear
Poruthoor 2013 [23]	Unclear	High	High	High	High
BenTaieb 2015 [24]	Unclear	Unclear	Low	High	High
BenTaieb 2016 [25]	Unclear	High	Unclear	High	High
BenTaieb 2017 [26]	Unclear	Unclear	Low	High	High
Lorsakul 2017 [27]	Unclear	Unclear	High	High	High
Du 2018 [28]	Unclear	Unclear	Unclear	Unclear	Unclear
Heindl 2018 [29]	Unclear	Low	Low	High	High
Kalra 2020 [30]	Unclear	Low	Low	High	High
Levine 2020 [31]	Unclear	Low	Low	Unclear	Unclear
Yaar 2020 [32]	Unclear	Unclear	Low	High	High
Yu 2020 [33]	Unclear	Low	Low	High	High
Gentles 2021 [34]	High	Unclear	High	High	High
Ghoniem 2021 [35]	Unclear	Unclear	Unclear	High	High
Jiang 2021 [36]	High	High	Unclear	High	High
Laury 2021 [37]	Low	High	High	High	High
Paijens 2021 [38]	Low	High	Unclear	High	High
Shin 2021 [39]	Unclear	Unclear	Unclear	High	High
Zeng 2021 [40]	Unclear	Unclear	Low	High	High
Boehm 2022 [41]	Unclear	High	Unclear	High	High
Boschman 2022 [42]	Unclear	Low	Low	High	High
Elie 2022 [43]	Unclear	Low	High	High	High
Farahani 2022 [44]	Unclear	Unclear	Low	Unclear	Unclear
Hu 2022 [45]	Unclear	Unclear	Unclear	Unclear	Unclear
Jiang 2022 [46]	Unclear	Unclear	High	High	High
Kasture 2022 [47]	High	High	High	High	High
Kowalski 2022 [48]	Unclear	Unclear	Unclear	High	High
Lazard 2022 [49]	Unclear	Unclear	Unclear	Unclear	Unclear
Liu 2022 [50]	Unclear	Unclear	Unclear	Unclear	Unclear
Mayer 2022 [51]	Unclear	Unclear	High	High	High
Nero 2022 [52]	Unclear	Low	High	High	High
Salguero 2022 [53]	Unclear	Unclear	Low	High	High
Wang 2022(a) [54]	Unclear	Unclear	Unclear	High	High
Wang 2022(b) [55]	Unclear	Unclear	Low	High	High
Yokomizo 2022 [56]	Low	Low	Unclear	Unclear	Unclear
Ho 2023 [57]	Unclear	Unclear	Unclear	High	High
Meng 2023 [58]	Unclear	Unclear	Low	High	High
Ramasamy 2023 [59]	High	High	High	High	High
Wang 2023 [60]	Unclear	Unclear	Unclear	High	High
Wu 2023 [61]	Unclear	Unclear	Low	High	High

**Table 1.** PROBAST risk of bias assessment results for the 45 papers included in this review. This is presented as one row for each paper because every paper that contained multiple models of interest was found to have the same risk of bias for every model.

## Data Synthesis Results

### Data in Included Literature

The number of participants in internal datasets varied by orders of magnitude, with each study including 1 to 776 ovarian cancer patients, and one study including over 10,000 total patients across a range of 32 malignancies [30]. Most research only used data from the five most common subtypes of ovarian carcinoma, though one recent study included the use of sex cord-stromal tumours [58]. Only one study explicitly included any prospective data collection, and this was only for a small subset which was not used for external validation [41].

As shown in Figure 3, the number of pathology slides used was often much greater than the number of patients included, with three studies using over 1000 slides from ovarian cancer patients [22, 33, 50]. In most of the studies, model development samples were WSIs containing resected or biopsied tissue (34/45), with others using individual tissue microarray (TMA) core images (5/45) or pre-cropped digital pathology images (3/45). Most studies used H&E-stained tissue (33/45) and others used a variety of IHC stains (11/45), with no two papers reporting the use of the same IHC stains. Some studies included multi-modal approaches, using genomics [23, 32, 35, 40, 41], proteomics [23, 40], transcriptomics [40], and radiomics [41] data alongside histopathological data.

The most commonly used data source was The Cancer Genome Atlas (TCGA) (18/45), a project from which over 30,000 digital pathology images from 33 malignancies are publicly available. The ovarian cancer subset, TCGA-OV [62], contains 1481 WSIs from 590 cases of ovarian serous carcinoma (mostly, but not exclusively, high-grade), with corresponding genomic, transcriptomic, and clinical data. This includes slides from eight data centres in the United States, with most slides containing frozen tissue sections (1374/1481) rather than formalin-fixed, paraffin-embedded (FFPE) sections. Other recurring data sources were the University of British Columbia Ovarian Cancer Research Program (OVCARE) repository [31, 42, 44], the Transcanadian study [24, 25], and clinical records at the Mayo Clinic [36, 46], Tri-Service General Hospital [54, 55, 60], and Memorial Sloan Kettering Cancer Center [41, 57]. All other researchers either used a unique data source (12/45) or did not report the provenance of their data (8/45). TCGA-OV, OVCARE, and the Transcanadian study are all multi-centre datasets. Aside from these, few studies reported the use of multi-centre data [38, 39, 40, 41, 44, 51]. Only two studies reported the use of multiple slide scanners, with every slide scanned on one of two available scanners [42, 44]. The countries from which data were sourced included Canada, China, Finland, France, Germany, Italy, Japan, the Netherlands, South Korea, Taiwan, the United Kingdom, and the United States of America.

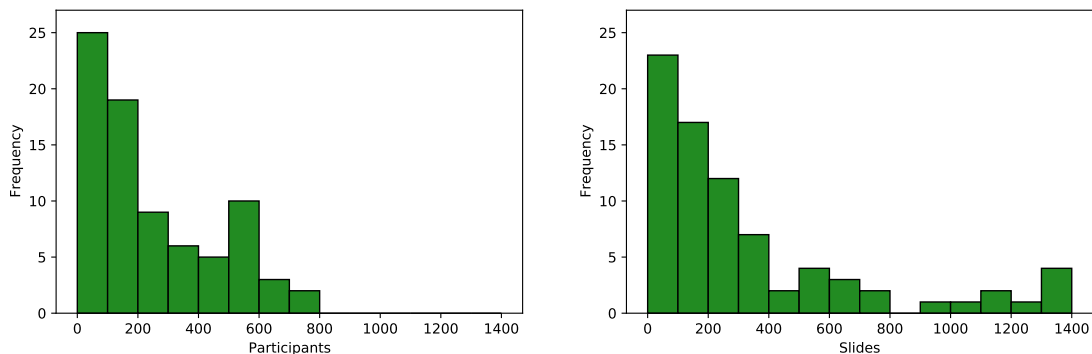


**Figure 3.** Histograms showing the number of ovarian cancer patients and slides used in model development. Many of these values are uncertain due to incomplete reporting, as reflected in Table 3.

### Methods in Included Literature

There was a total of 80 models of interest in the 45 included papers, with each paper containing 1 to 6 such models. There were 37 diagnostic models, 22 prognostic models, and 21 other models predicting diagnostically relevant information. Diagnostic model outcomes included the classification of malignancy status (10/37), histological subtype (7/37), primary cancer type (5/37),



genetic mutation status (4/37), tumour-stroma reaction level (3/37), grade (2/37), transcriptomic subtype (2/37), stage (1/37), microsatellite instability status (1/37), epithelial-mesenchymal transition status (1/37), and homologous recombination deficiency status (1/37). Prognostic models included the prediction of treatment response (11/23), overall survival (6/23), progression-free survival (3/23), and recurrence (2/23). The other models performed tasks which could be used to assist pathologists in analysing pathology images, including measuring the quantity/intensity of staining, generating segmentation masks, and classifying tissue/cell types.

A variety of models were used, with the most common types being convolutional neural network (CNN) (41/80), support vector machine (SVM) (10/80), and random forest (6/80). CNN architectures included GoogLeNet [28], VGG16 [33, 46], VGG19 [31, 44], InceptionV3 [39, 54, 55, 60], ResNet18 [41, 42, 44, 45, 49, 51], ResNet34 [56], ResNet50 [52, 58, 61], ResNet182 [57], and MaskRCNN [46]. Novel CNNs typically used multiple standardised blocks involving convolutional, normalization, activation, and/or pooling layers [32, 47, 48], with two studies also including attention modules [50, 60]. One study generated their novel architecture by using a topology optimization approach on a standard VGG16 [35].

Most researchers split their original images into patches to be separately processed, with patch sizes ranging from 60x60 to 2048x2048 pixels, the most common being 512x512 pixels (19/56) and 256x256 pixels (12/56). A range of feature extraction techniques were employed, including both hand-crafted/pre-defined features (23/80) and features that were automatically learned by the model (51/80). Hand-crafted features included a plethora of textural, chromatic, and cellular and nuclear morphological features. Hand-crafted features were commonly used as inputs to classical ML methods, such as SVM and random forest models. Learned features were typically extracted using a CNN, which was often also used for classification.

Despite the common use of patches, most models made predictions at the WSI level (29/80), TMA core level (18/80), or patient level (6/80), requiring aggregation of patch-level information. Two distinct aggregation approaches were used, one aggregating before modelling and one aggregating after modelling. The former approach requires the generation of slide-level features before modelling, the latter requires the aggregation of patch-level model outputs to make slide-level predictions. Slide-level features were generated using summation [58], averaging [23, 40, 57], attention-based weighted averaging [45, 50, 52, 49, 61], concatenation [25, 30], as well as more complex embedding approaches using Fisher vector encoding [24] and k-means clustering [26]. Patch-level model outputs were aggregated to generate slide-level predictions by taking the maximum [32, 60], median [56], or average [35], using voting strategies [42, 55], or using a random forest classifier [44]. These approaches are all examples of *multiple instance learning* (MIL), though few models of interest were reported using this terminology [32, 45, 49, 52].

Publication	Ovarian Cancer Data Source	Models of Interest	Outcome Type	Model Outcomes	Published Code
Dong 2010(a) [17]	Unclear	1	Other	Stain segmentation	None
Dong 2010(b) [18]	Unclear	1	Other	Stain segmentation	None
Signolle 2010 [19]	Unclear	1	Other	Tumour segmentation	None
Janowczyk 2011 [20]	Unclear	1	Diagnosis	Malignancy	None
Janowczyk 2012 [21]	Unclear	1	Other	Stain segmentation	None
Kothari 2012 [22]	TCGA-OV (Multi-city, USA)	1	Diagnosis	Malignancy	None
Poruthoor 2013 [23]	TCGA-OV (Multi-city, USA)	2	Diagnosis, Prognosis	Grade; Overall survival	None
BenTaieb 2015 [24]	Transcanadian Study (Multi-city, Canada)	1	Diagnosis	Histological subtype	None
BenTaieb 2016 [25]	Transcanadian Study (Multi-city, Canada)	1	Diagnosis	Histological subtype	Inaccessible
BenTaieb 2017 [26]	Unclear	1	Diagnosis	Histological subtype	Inaccessible
Lorsakul 2017 [27]	Unclear	1	Other	Cell type	None
Du 2018 [28]	Unique (Oklahoma, USA)	1	Other	Tissue type	None
Heindl 2018 [29]	TCGA-OV (Multi-city, USA)	1	Other	Cell type	<a href="https://yuanlab.org/file/Ov3sweave2.pdf">https://yuanlab.org/file/Ov3sweave2.pdf</a>
Kalra 2020 [30]	TCGA-OV (Multi-city, USA)	4	Diagnosis	Primary cancer type	None
Levine 2020 [31]	OVCARE (Vancouver, Canada)	1	Diagnosis	Histological subtype	<a href="https://github.com/AIMLab-UBC/pathGAN">https://github.com/AIMLab-UBC/pathGAN</a>
Yaar 2020 [32]	TCGA-OV (Multi-city, USA)	1	Prognosis	Treatment response	<a href="https://github.com/asfandasfo/LUPI">https://github.com/asfandasfo/LUPI</a>
Yu 2020 [33]	TCGA-OV (Multi-city, USA)	4	Diagnosis, Prognosis	Malignancy, Grade, Transcriptomic subtype; Treatment response	<a href="https://github.com/khyu/ovarian_ca/">https://github.com/khyu/ovarian_ca/</a>
Gentles 2021 [34]	Unique (Newcastle, UK)	6	Other	Stain quantity/intensity	None
Ghoniem 2021 [35]	TCGA-OV (Multi-city, USA)	1	Diagnosis	Stage	None
Jiang 2021 [36]	Mayo Clinic (Rochester, USA)	1	Diagnosis	Malignancy	<a href="https://github.com/smuiang/CellularComposition">https://github.com/smuiang/CellularComposition</a>
Laury 2021 [37]	Unique (Helsinki, Finland)	1	Prognosis	Progression-free survival	None
Pajens 2021 [38]	Unique (Groningen & Zwolle, The Netherlands)	1	Other	Tissue type	None
Shin 2021 [39]	TCGA-OV (Multi-city, USA) + Unique (Ajou, Korea)	1	Diagnosis	Malignancy	<a href="https://github.com/ABMI/HistopathologyStyleTransfer">https://github.com/ABMI/HistopathologyStyleTransfer</a>
Zeng 2021 [40]	TCGA-OV (Multi-city, USA) + Unique (Shanghai, China)	5	Diagnosis, Prognosis	Genetic mutation, Transcriptomic subtype, Microsatellite instability; Overall survival	None
Boehm 2022 [41]	TCGA-OV (Multi-city, USA) + MSKCC (New York, USA)	3	Diagnosis, Prognosis	Malignancy; Overall survival, Progression-free survival	<a href="https://github.com/kmboehm/onco-fusion">https://github.com/kmboehm/onco-fusion</a>
Boschman 2022 [42]	OVCARE (Vancouver, Canada)	1	Diagnosis	Histological subtype	None
Elie 2022 [43]	Unique (Caen, France)	3	Other	Stain quantity/intensity	None
Farahani 2022 [44]	OVCARE (Vancouver, Canada) + Unique (Calgary, Canada)	2	Diagnosis	Malignancy, Histological subtype	<a href="https://github.com/AIMLab-UBC/ModernPath2022">https://github.com/AIMLab-UBC/ModernPath2022</a>
Hu 2022 [45]	TCGA-OV (Multi-city, USA)	1	Diagnosis	Epithelial-mesenchymal transition	<a href="https://github.com/superhy/LCSB-MIL">https://github.com/superhy/LCSB-MIL</a>
Jiang 2022 [46]	Mayo Clinic (Rochester, USA)	4	Diagnosis, Other	Tumour-stroma reaction; Tumour segmentation	<a href="https://github.com/smuiang/TumorStromaReaction">https://github.com/smuiang/TumorStromaReaction</a>
Kasture 2022 [47]	TCGA-OV* (Multi-city, USA)	1	Diagnosis	Histological subtype	<a href="https://github.com/kokilakasture/OvarianCancerPrediction">https://github.com/kokilakasture/OvarianCancerPrediction</a>
Kowalski 2022 [48]	Unclear	1	Other	Tumour segmentation	None
Lazard 2022 [49]	TCGA-OV (Multi-city, USA)	1	Diagnosis	Homologous recombination deficiency status	<a href="https://github.com/trislaz/wsi_mil">https://github.com/trislaz/wsi_mil</a>
Liu 2022 [50]	TCGA-OV (Multi-city, USA)	1	Prognosis	Overall survival	<a href="https://github.com/RanSuLab/EOCprognosis">https://github.com/RanSuLab/EOCprognosis</a>
Mayer 2022 [51]	TCGA-OV (Multi-city, USA) + Unique (Frankfurt, Germany)	1	Diagnosis	Malignancy	None
Nero 2022 [52]	Unique (Rome, Italy)	2	Diagnosis, Prognosis	Genetic mutation; Relapse	None
Salguero 2022 [53]	TCGA-OV (Multi-city, USA)	1	Diagnosis	Malignancy	None
Wang 2022(a) [54]	Tri-Service (Taipei, Taiwan)	4	Prognosis	Treatment response	None
Wang 2022(b) [55]	Tri-Service (Taipei, Taiwan)	1	Prognosis	Treatment response	None
Yokomizo 2022 [56]	Unique (Tokyo, Japan)	3	Prognosis	Overall survival, Progression-free survival, Relapse	Inaccessible
Ho 2023 [57]	MSKCC (New York, USA)	2	Diagnosis, Other	Genetic mutation; Tumour segmentation	<a href="https://github.com/MSKCC-Computational-Pathology/DMMN-ovary">https://github.com/MSKCC-Computational-Pathology/DMMN-ovary</a>
Meng 2023 [58]	Unique (Beijing, China)	1	Diagnosis	Malignancy	<a href="https://github.com/dreambamboo/STT-BOX-public">https://github.com/dreambamboo/STT-BOX-public</a>
Ramasamy 2023 [59]	TCGA-OV* (Multi-city, USA)	2	Diagnosis, Other	Primary cancer type; Tumour segmentation	None
Wang 2023 [60]	Tri-Service (Taipei, Taiwan)	4	Prognosis	Treatment response	<a href="https://github.com/cwwang1979/OvaryTreatment_AnginPKM2VEGF">https://github.com/cwwang1979/OvaryTreatment_AnginPKM2VEGF</a>
Wu 2023 [61]	TCGA-OV (Multi-city, USA)	1	Prognosis	Overall survival	None

**Table 2.** Characteristics of the 45 studies included in this systematic review. Details are shown for individual models in Table 3. Six data sources are used in multiple studies - The Cancer Genome Atlas (TCGA-OV) [62], the British Columbia Ovarian Cancer Research Program (OVCARE), The Transcanadian Study [63], and three individual centres (Mayo Clinic, Tri-Service, and Memorial Sloan Kettering Cancer Center (MSKCC)). Code is labelled as inaccessible where it could not be found despite a link being provided in the publication. \*Indicates papers where significant discrepancies were found regarding the data source, as described in the Discussion.

Diagnosis Outcome	Publication	Internal Path. Images	Internal Path. Images Data*	Other Data*	Stain Type	Original Image Size	Patch Size (pixels)	Magnifications	Feature Extraction	Histopathological Features	Final Model	Prediction precision	Classes	Validation Type (and number of repeats)	External validation data	Metric	Internal Results	Internal Variability (measure)	External Results	External Variability (measure)	
Malignancy Status	Jamowczyk 2011 [20]	6	11		IHC	1400x1400	Unclear	40x	Hand-crafted	Texture, cellular morphology	Probabilistic Boosting Tree	Patch	2 - Tumour, stroma	Monte Carlo cross-validation (5 reps)		AUC	0.8341				
	Kothari 2012 [21]	171	130		H&E	WSI	512x512	Unclear	Hand-crafted	Colour, texture, cellular and nuclear morphology	SVM	Patch	2 - Tumour, non-tumour	Single train/test split		Accuracy	90%				
	Yu 2020 [33]	587	1375		H&E	WSI	Unclear	Unclear	Learned	CNN features (VGG16)	CNN (VGG16)	WSI	2 - Malignant, benign	Monte Carlo cross-validation (3 reps)		AUC	0.975	±0.001 (unclear)			
	Jiang 2021 [36]	30	230		H&E	WSI	512x512	40x	Hand-crafted	Colour, cellular and nuclear morphology	SVM	WSI	2 - HGSC, Serous borderline tumour	Unclear		Accuracy	90.64%				
	Shin 2021 [39]	143	≥142		H&E	WSI	256x256	Unclear	Learned	CNN features (Inception V3)	CNN (Inception V3)	Patch	2 - Cancer, non-cancer	External validation	32 WSIs from different centre	Accuracy	0.96		80.8%		
	Boehm 2022 [41]	283	2283		H&E	WSI	128x128	Unclear	Learned	CNN features (ResNet18)	CNN (ResNet18)	Patch	4 - Tumour, stroma, fat, necrosis	4-fold cross-validation		Accuracy	88%				
	Farahani 2022 [44]	2416	416		H&E	WSI	512x512	20x	Learned	CNN features (ResNet18)	CNN (ResNet18)	Patch	2 - Tumour, stroma	3-fold cross-validation		Balanced accuracy	96.99%				
	Mayer 2022 [51]	101	101		H&E	WSI	512x512	Unclear	Learned	CNN features (ResNet18)	CNN Ensemble (ResNet18)	Patch	2 - Cancer, non-cancer	Monte Carlo cross-validation (10 reps) & external validation	41 WSIs from different centre	Accuracy per patient	56.3%-93.2%	Unclear plot (IQR & range)	Unclear plot (IQR & Range)		
	Salguero 2022 [53]	18	≥18		H&E	WSI	100x100	40x	Hand-crafted	Colour, texture, cellular morphology	SVM	WSI	2 - Cancer, non-cancer	Single train/test split		Accuracy	73%				
	Meng 2023 [58]	80	94		H&E	WSI	512x512	Unclear	Learned	CNN features (ResNet50)	CNN (novel ST-BOX)	WSI	2 - Malignant, benign	3-fold cross-validation (non-ovarian) & external validation (ovarian)	50 WSIs from 30 patients	AUC per subtype	0.9815-0.9953		0.8883		
Histological Subtype	BenTaieb 2015 [24]	80	80		H&E	WSI	Unclear	20x, 30x	Learned	CNN features (deconvolution network)	SVM	WSI	5 - HGSC, LGSC, CCC, MC, EC	Monte Carlo cross-validation (3 reps)		Accuracy	91.0%	±1.0% (unclear)			
	BenTaieb 2016 [25]	80	80		H&E	WSI	500x500	20x, 40x	Hand-crafted	Colour, texture, cellular morphology, cytology	SVM	WSI	5 - HGSC, LGSC, CCC, MC, EC	Leave-one-patient-out cross-validation (5 reps)		Accuracy	95.0%	±1.5% (one SD)			
	BenTaieb 2017 [26]	133	133		H&E	WSI	500x500	4x, 10x, 20x, 40x	Learned	CNN features (novel K-means)	SVM	WSI	5 - HGSC, LGSC, CCC, MC, EC	Single train/test split		Accuracy	90%				
	Levine 2020 [31]	406	406		H&E	WSI	256x256	40x	Learned	CNN features (VGG19)	CNN (VGG19)	Patch	5 - HGSC, LGSC, CCC, MC, EC	Monte Carlo cross-validation (10 reps)		Accuracy	70.87%	±6.35% (one SD)			
	Boschman 2022 [42]	160	308		H&E	WSI	256x256	20x	Learned	CNN features (ResNet18)	CNN (ResNet18)	WSI	5 - HGSC, LGSC, CCC, MC, EC	External validation	60 WSIs from different centre	Accuracy	75.15%	±10.44% (one SD)	0.94		
	Farahani 2022 [44]	485	948		H&E	WSI	512x512	20x	Learned	CNN features (VGG19)	CNN (VGG19)	WSI	5 - HGSC, LGSC, CCC, MC, EC	3-fold cross-validation & external validation	60 WSIs from different centre	Balanced accuracy	81.38%		80.97%		
	Kasture 2022 [47]	500	500		H&E	WSI	227x227	NA	20x	Learned	CNN features (novel KX-Net)	CNN (novel KX-Net)	Patch	5 - Serous, MC, CCC, EC, Non-cancer	10-fold cross-validation		Accuracy	0.9475		0.9469	
																Accuracy	91%				
Primary Cancer Type	Kaira 2020 [30]	933	1039		H&E	WSI	1000x1000	20x	Learned	NNS features (unclear architectures)	Yottsel Search	WSI	4 - Ovarian, uterine carcinosarcoma, uterine endometrial, cervical (FFPE slides)	Leave-one-patient-out cross-validation		Accuracy (Ovarian)	66.98%				
	Kaira 2020 [30]	1450	2216		H&E	WSI	1000x1000	20x	Learned	NNS features (unclear architectures)	Yottsel Search	WSI	4 - Ovarian, uterine carcinosarcoma, uterine endometrial, cervical (frozen slides)	Leave-one-patient-out cross-validation		Accuracy (Ovarian)	98.98%				
	Kaira 2020 [30]	9,484	11,561		H&E	WSI	1000x1000	20x	Learned	NNS features (unclear architectures)	Yottsel Search	WSI	13 - Gynaecological, brain, pulmonary, prostate/testis, breast, ... (FFPE slides)	Leave-one-patient-out cross-validation		Accuracy (Gynaecological)	68.86%				
	Kaira 2020 [30]	100,000	120,000		H&E	WSI	1000x1000	20x	Learned	NNS features (unclear architectures)	Yottsel Search	WSI	13 - Gynaecological, brain, pulmonary, prostate/testis, breast, ... (frozen slides)	Leave-one-patient-out cross-validation		Accuracy (Gynaecological)	68.86%				
	Ramasamy 2023 [59]	2776	776		Unclear	WSI	Unclear	Unclear	Learned	CNN features (novel architecture)	CNN (novel)	WSI	2 - ovarian cancer, non-ovarian cancer	5-fold cross-validation		Accuracy	99.2%				
	Zeng 2021 [40]	229	2229		H&E	WSI	1000x1000	Unclear	Hand-crafted	Texture, cellular and nuclear morphology	Random Forest	Patient	2 - BRCA1 Mutated, not mutated	Single train/test split		AUC	0.952				
	Zeng 2021 [40]	229	2229		H&E	WSI	1000x1000	Unclear	Hand-crafted	Texture, cellular and nuclear morphology	Random Forest	Patient	2 - BRCA2 Mutated, not mutated	Single train/test split		AUC	0.912				
	Nero 2022 [52]	664	664		H&E	WSI	256x256	Unclear	Learned	CNN features (ResNet50)	CNN (CLAM)	WSI	2 - BRCA1/2 Mutated, wild-type	Single train/test split		Accuracy	0.58				
	HO 2023 [57]	609	609		H&E	WSI	224x224	5x	Learned	CNN features (ResNet18)	CNN (ResNet18)	Patch	2 - BRCA1/2 Mutated, wild-type	Single train/test split		AUC	0.43				
	Tumour-Stroma Reaction	Jiang 2022 [46]	306	306		H&E	WSI	256x256	Unclear	Learned	CNN features (Mask-RCNN)	CNN (VGG16)	Patch	3 - Low, intermediate, high (fibrosis score)	Single train/test split		Sensitivity per class	0.91-0.93			
Jiang 2022 [46]		306	306		H&E	WSI	256x256	Unclear	Learned	CNN features (Mask-RCNN)	CNN (VGG16)	Patch	3 - Low, intermediate, high (cellularity score)	Single train/test split		Sensitivity per class	0.79-0.95				
Jiang 2022 [46]		306	306		H&E	WSI	256x256	Unclear	Learned	CNN features (Mask-RCNN)	CNN (VGG16)	Patch	3 - Low, intermediate, high (orientation score)	Single train/test split		Sensitivity per class	0.74-0.95				
Poruthottu 2013 [23]		387	2387		H&E	WSI	512x512	Unclear	Hand-crafted	Colour, texture, cellular and nuclear morphology	SVM	WSI	2 - Grade 1-2, Grade 3-4	Monte Carlo cross-validation (15 reps)		Accuracy	88%	Unclear plot (one SD)			
Yu 2020 [33]		180	180		H&E	WSI	Unclear	Unclear	Learned	CNN features (VGG16)	CNN (VGG16)	WSI	2 - Low to moderate risk	Monte Carlo cross-validation (3 reps)		Accuracy	0.813	±0.088 (unclear)			
Yu 2020 [33]		553	51341		H&E	WSI	Unclear	Unclear	Learned	CNN features (VGG16)	CNN (VGG16)	WSI	4 - Proliferative, differentiated, immunoreactive, mesenchymal	5-fold cross-validation		p-value	<0.001				
Zeng 2021 [40]		229	2229		H&E	WSI	1000x1000	Unclear	Hand-crafted	Texture, cellular and nuclear morphology	Random Forest	Patient	4 - Proliferative, differentiated, immunoreactive, mesenchymal	Single train/test split		AUC per class	0.918-0.961				
Stage		Ghoniem 2021 [35]	587	587	G	H&E	WSI	224x224	Unclear	Learned	CNN features (altered VGG16)	CNN (altered VGG16)	WSI	5 - I, II, III, IV, Not available	5-fold cross-validation (20 reps)		Accuracy	98.87%			
Microsatellite Instability		Zeng 2021 [40]	229	2229		H&E	WSI	1000x1000	Unclear	Hand-crafted	Texture, cellular and nuclear morphology	Random Forest	Patient	3 - High instability, stable, NA	Single train/test split		AUC (High instability)	0.919			
Epithelial-Mesenchymal Transition Status		Hu 2022 [45]	470	70		H&E	WSI	256x256	40x	Learned	CNN features (ResNet18)	CNN (novel adlinter-MIL)	WSI	2 - High, low	Monte Carlo cross-validation (10 reps)		Balanced accuracy	85.45%	±0.48% (variance)		
																AUC	0.7455	±0.0043 (variance)			
HRD Status	Lazard 2022 [49]	190	90		H&E	WSI	224x224	20x	Learned	CNN features (ResNet18)	NN	WSI	2 - Homologous Recombination Deficient, Proficient	Unclear		AUC	0.73				
Prognosis Outcome	Publication	Internal Path. Images	Internal Path. Images Data*	Other Data*	Stain Type	Original Image Size	Patch Size (pixels)	Magnifications	Feature Extraction	Histopathological Features	Final Model	Prediction precision	Classes	Validation Type (and number of repeats)	External validation data	Metric	Internal Results	Internal Variability (measure)	External Results	External Variability (measure)	
	Year 2020 [32]	220	2220	G	H&E	WSI	512x512	20x	Learned	CNN features (novel)	CNN	WSI	2 - Chemo-resistant, chemo-sensitive	5-fold cross-validation		Accuracy	0.79	±0.07 (one SD)			
	Yu 2020 [33]	277	≤1065		H&E	WSI	Unclear	Unclear	Learned	CNN features (VGG16)	CNN (VGG16)	WSI	2 - Early relapse, late relapse	5-fold cross-validation		p-value	0.003				
	Wang 2022(a) [54]	180	180	IHC	TMA	512x512	20x	Learned	CNN features (modified Inception V3)	CNN (modified Inception V3)	TMA	WSI	2 - Effective, invalid (AM2 stain)	5-fold cross-validation		AUC	0.91	±0.05 (unclear)			
	Wang 2022(a) [54]	180	180	TMA	512x512	20x	Learned	CNN features (modified Inception V3)	CNN (modified Inception V3)	TMA	WSI	2 - Effective, invalid (C3 stain)	5-fold cross-validation		AUC	0.78	±0.12 (unclear)				
	Wang 2022(a) [54]	180	180	IHC	TMA	512x512	20x	Learned	CNN features (modified Inception V3)	CNN (modified Inception V3)	TMA	WSI	2 - Effective, invalid (C5 stain)	5-fold cross-validation		AUC	0.66	±0.07 (unclear)			
	Wang 2022(a) [54]	180	180	IHC	TMA	512x512	20x	Learned	CNN features (modified Inception V3)	CNN (modified Inception V3)	TMA	WSI	2 - Effective, invalid (NRP3 stain)	5-fold cross-validation		AUC	0.55	±0.08 (unclear)			
	Wang 2022(b) [55]	78	288		H&E	WSI	512x512	Unclear (multiple)	Learned	CNN features (Inception V3)	CNN (Inception V3)	WSI	2 - Effective, invalid	5-fold cross-validation & external validation	175 TMAs from 71 patients	Accuracy	88.2%	±6% (unclear)	77.5%		
	Wang 2023 [60]	180	180	IHC	TMA	512x512	20x	Learned	CNN features (novel)	CNN (InceptionV3)	TMA	WSI	2 - Effective, invalid (PKM2 stain)	5-fold cross-validation		AUC	0.99	±0.01 (unclear)			
	Wang 2023 [60]	180	180	IHC	TMA	512x512	20x	Learned	CNN features (novel)	CNN (InceptionV3)	TMA	WSI	2 - Effective, invalid (Ang-2 stain)	5-fold cross-validation		AUC	1.00	±0.01 (unclear)			
Wang 2023 [60]	180	180	IHC	TMA	512x512	20x	Learned	CNN features (novel)	CNN (InceptionV3)	TMA	WSI	2 - Effective, invalid (VEGF stain)	5-fold cross-validation		AUC	0.89	±0.08 (unclear)				
Overall Survival	Poruthottu 2013 [23]	387	2387		H&E	WSI	512x512	Unclear	Hand-crafted	Colour, texture, cellular and nuclear morphology	CNN Ensemble (InceptionV3)	TMA	2 - Effective, invalid (PKM2+Ang-2 stain)	5-fold cross-validation		Accuracy	1.00	±0.00 (unclear)			
	Zeng 2021 [40]	229	2229	G,P,T	H&E	WSI	1000x1000	Unclear	Hand-crafted	Texture, cellular and nuclear morphology	Random Forest	Patient	2 - High risk, low risk	Monte Carlo cross-validation (15 reps)		Accuracy	95%	Unclear plot (one SD)			
																External validation	TMAs from 92 patients	Hazard ratio	18.23	10.34-34.38 (95% CI)	
																	p-value	<0.001		0.0097	
	Boehm 2022 [41]	444	2283	R	H&E	WSI	128x128	Unclear	Hand-crafted	Colour, texture, cellular and nuclear morphology	Cox model	WSI	Risk score	Single train/test split		C-index	0.61	0.594-0.625 (95% CI)			
	Ugo 2022 [60]	383	3286		H&E	WSI	512x512	20x	Learned	CNN features (novel DeepConvAttention(Surv))	CNN (novel DCAS)	Patient	Risk score	Single train/test split		C-index	0.38	±0.008 (unclear)			
	Yokomizo 2022 [56]	110	2110		H&E	WSI	255x255	Unclear	Learned	CNN features (ResNet34)	CNN (ResNet34)	TMA	TMA	Monte Carlo cross-validation (10 reps)		AUC	0.95				
	Wu 2023 [61]	90	90		H&E	WSI	256x256	Unclear	Learned	CNN features (ResNet50)	CNN (CLAM)	WSI	Risk score	5-fold cross-validation		C-index	0.5789	0.5096-0.6053 (CI range)			
	Laury 2011 [37]	52	227		H&E	WSI	Unclear	Unclear	Learned	CNN features (unclear architecture)	NN	WSI	2 - <6 months, ≥18 months	Single train/test split		Accuracy	82%				
	Boehm 2022 [41]	422	2261	G,R	H&E	WSI	128x128	Unclear	Hand-crafted	Colour, texture, cellular and nuclear morphology	Cox model	WSI	2 - High, low	Single train/test split		p-value	0.040				
Yokomizo 2022 [56]	110	2110		H&E	WSI	255x255	Unclear	Learned	CNN features (ResNet34)	CNN (ResNet34)	TMA	TMA	Monte Carlo cross-validation (10 reps)		Accuracy	0.98					
Relapse	Nero 2022 [52]	656	656		H&E	WSI	256x256	Unclear	Learned	CNN features (ResNet50)	CNN (CLAM)	WSI	2 - Relapse/progression, no relapse/progression	Single train/test split		AUC	0.714				
	Yokomizo 2022 [56]	110	2110		H&E	WSI	255x255	Unclear	Learned	CNN features (ResNet34)	CNN (ResNet34)	TMA	2 - Recurrent, non-recurrent	Monte Carlo cross-validation (10 reps)		AUC	0.98				
Other Outcome	Publication	Internal Path. Images	Internal Path. Images Data*	Other Data*	Stain Type	Original Image Size	Patch Size (pixels)	Magnifications	Feature Extraction	Histopathological Features	Final Model	Prediction precision	Classes	Validation Type (and number of repeats)	External validation data	Metric	Internal Results	Internal Variability (measure)	External Results	External	

Most studies included segmentation at some stage, with many of these analysing tumour/stain segmentation as a model outcome [17, 18, 19, 20, 21, 38, 46, 48, 57, 59]. Some other studies used segmentation to determine regions of interest for further modelling, either simply separating tissue from background [22, 30, 52, 61], or using tumour segmentation to select the most relevant tissue regions [34, 37, 54, 55, 60]. One study also used segmentation to detect individual cells for classification [29]. Some studies also used segmentation in determining hand-crafted features relating to the quantity and morphology of different tissues, cells, and nuclei [22, 23, 25, 36, 40, 41].

While attention-based approaches have been applied to other malignancies for several years [64, 65], they were only seen in the most recent ovarian cancer studies [44, 45, 49, 50, 52, 54, 55, 61, 60], and none of the methods included self-attention, an increasingly popular method for other malignancies [66]. Most models were deterministic, though hidden Markov trees [19], probabilistic boosting trees [20], and Gaussian mixture models [43] were also used. Aside from the common use of low-resolution images to detect and remove non-tissue areas, images were typically analysed at a single resolution, with only six papers including multi-magnification techniques in their models of interest. Four of these combined features from different resolutions for modelling [24, 25, 26, 57], and the other two used different magnifications for selecting informative tissue regions and for modelling [54, 55]. Out of the papers for which it could be determined, the most common modelling magnifications were 20x (35/41) and 40x (7/41). Few models integrated histopathology data with other modalities (6/80). Multi-modal approaches included the concatenation of separately extracted uni-modal features before modelling [23, 35, 40], the amalgamation of uni-modal predictions from separate models [41], and a teacher-student approach where multiple modalities were used in model training but only histopathology data was used for prediction [32].

#### ***Analysis in Included Literature***

Analyses were limited, with less than half of the model outcomes being evaluated with cross-validation (39/80) and with very few externally validated using independent ovarian cancer data (7/80), despite small internal cohort sizes. Cross-validation methods included k-fold (22/39) with 3 to 10 folds, Monte Carlo (12/39) with 3 to 15 repeats, and leave-one-patient-out cross-validations (5/39). Some other papers included cross-validation on the training set to select hyperparameters but used only a small unseen test set from the same data source for evaluation. Externally validated models were all trained with WSIs, with validations either performed on TMA cores (2/7) or WSIs from independent data sources (5/7), with two of these explicitly using different scanners to digitize internal and external data [42, 44]. Some reported methods were externally validated with data from non-ovarian malignancies, but none of these included ovarian cancer data in any capacity, so were not included in the review. However, there was one method which trained with only gastrointestinal tumour data and externally validated with ovarian tumour data [58].

Most classification models were evaluated using accuracy, balanced accuracy, and/or area under the receiver operating characteristic curve (AUC), with one exception where only a p-value was reported measuring the association between histological features and transcriptomic subtypes based on a Kruskal-Wallis test [33]. Some models were also evaluated using the F1-score, which we chose not to tabulate (in Figure 3) as the other metrics were reported more consistently. Survival model performance was typically reported using AUC, with other metrics including p-value, accuracy, hazard ratios, and C-index, which is similar to AUC but can account for censoring. Segmentation models were almost all evaluated differently from each other, with different studies reporting AUC, accuracy, Dice coefficient, intersection over union, sensitivity, specificity, and qualitative evaluations. Regression models were all evaluated using the coefficient of determination ( $R^2$ -statistic). For some models, performance was broken down per patient [43, 51], per subtype [58], or per class [29, 30, 40, 46], without an aggregated, holistic measure of model performance.

The variability of model performance was not frequently reported (33/94), and when it was reported it was often incomplete. This included cases where it was unclear what the intervals represented (95% confidence interval, one standard deviation, variation, etc.), or not clear what the exact bounds of the interval were due to results being plotted but not explicitly stated. Within the entire review, there were only three examples in which variability was reported during external validation [39, 42, 51], only one of which clearly reported both the bounds and the type of the interval [39]. No studies performed any Bayesian form of uncertainty quantification. Reported results are shown in Table 3, though direct comparisons between the performance of different

models should be treated with caution due to the diversity of data and validation methods used to evaluate different models, the lack of variability measures, the consistently high risks of bias, and the heterogeneity in reported metrics.

## DISCUSSION

The vast majority of published research on AI for diagnostic or prognostic purposes in ovarian cancer histopathology was found to be at a high risk of bias due to issues within the analyses performed. Researchers often used a limited quantity of data and conducted analyses on a single train-test data split without using any methods to account for overfitting and model optimism (cross-validation, bootstrapping, external validation). These limitations are common in gynaecological AI research using other data types, with recent reviews pointing to poor clinical utility caused by predominantly retrospective studies using limited data [67, 68] and limited methodologies with weak validation, which risk model performance being overestimated [69, 70].

The more robust analyses included one study in which several relevant metrics were evaluated using 10 repeats of Monte Carlo cross-validation on a set of 406 WSIs, with standard deviations reported for each metric [31]. Other positive examples included the use of both internal cross-validation and external validation for the same outcome, giving a more rigorous analysis [44, 51, 55]. While external validations were uncommon, those which were conducted offered a real insight into model generalisability, with a clear reduction in performance on all external validation sets except one [44]. The only study which demonstrated high generalisability included the largest training set out of all externally validated approaches, included more extensive data labelling than many similar studies, and implemented a combination of three colour normalisation approaches, indicating that these factors may benefit generalisability.

Studies frequently had an unclear risk of bias within the participants and predictors domains of PROBAST due to incomplete reporting. Frequently missing information included where the patients were recruited, how many patients were included, how many samples/images were used, whether any patients/images were excluded, and the methods by which tissue was processed and digitized. Reporting was often poor regarding open-access datasets. Only three papers were found to be at low risk of bias for participants, with these including clear and reasonable patient recruitment strategies and selection criteria, which can be seen as positive examples for other researchers [37, 38, 56]. Information about the predictors (histopathology images and features derived thereof) was generally better reported, but still often missed key details which meant that it was unclear whether all tissue samples were processed similarly to avoid risks of bias from visual heterogeneity. It was found that when patient characteristics were reported, they often showed a high risk of bias. Many studies included very small quantities of patients with specific differences from the majority (e.g. less than 20 patients with a different cancer subtype to the majority), causing a risk of spurious correlations and results which are not generalisable to the wider population.

Reporting was particularly sparse in studies which used openly accessible data, possibly indicating that AI-focused researchers were not taking sufficient time to understand these datasets and ensure their research was clinically relevant. For example, many of the researchers who used TCGA data included frozen tissue sections without commenting on whether this was appropriate, despite the fact that pathologists do not consider them to be of optimal diagnostic quality. One paper handled TCGA data more appropriately, with a clear explanation of the positives and negatives of the dataset, and entirely separate models for FFPE and frozen slides [30].

Sharing code can help to mitigate the effects of incomplete reporting and drastically improve reproducibility, but only 19 of the 45 papers did this, with some of these appearing to be incomplete or inaccessible. The better code repositories included detailed documentation to aid reproducibility, including environment set-up information [33, 58], overviews of included functions [41, 49, 57], and code examples used to generate reported results [29].

Two papers were found to have major discrepancies between the reported data and the study design, indicating much greater risks of bias than those seen in any other research [47, 59]. In one paper [47], it was reported that TCGA-OV data was used for subtyping with 5 classes, despite this dataset only including high-grade serous and low-grade serous carcinomas. In the other paper [59], it was reported that TCGA-OV data was used for slide-level classification into ovarian

cancer and non-ovarian cancer classes using PAS-stained tissue, despite TCGA-OV only containing H&E-stained ovarian cancer slides.

### **Limitations of the Review**

While the review protocol was designed to reduce biases and maximise the quantity of relevant research included, there were some limitations. This review is restricted to published literature in the English language, however, AI research may be published in other languages or made available as pre-prints without publication in peer-reviewed journals, making this review incomplete. While most of the review process was completed by multiple independent researchers, the duplicate detection was performed by only a single researcher, raising the possibility of errors in this step of the review process, resulting in incorrect exclusions. Due to the significant time gap between the initial and final literature searches (approximately 12 months), there may have been inconsistencies in interpretations, both for data extraction and risk of bias assessments. Finally, this review focused only on light microscopy images of human histopathology samples relating to ovarian cancer, so may have overlooked useful literature outside of this domain.

### **Development of the Field**

The field of AI in ovarian cancer histopathology diagnosis is rapidly growing, with more research published since the start of 2020 than in all preceding years combined. The earliest research, published between 2010-2013, used hand-crafted features to train classical ML methods such as SVMs. These models were used for segmentation [17, 18, 19, 21], malignancy classification [20, 22], grading [23], and overall survival prediction [23]. Most of these early studies focused on IHC-stained tissue (5/7), which would be much less commonly used in subsequent research (6/38).

The field was relatively dormant in the following years, with only 6 papers published between 2014-2019, half of which had the same primary author [24, 25, 26]. These models still used traditional ML classifiers, though some used learned features rather than the traditional hand-crafted features. The models developed were used for histological subtyping [24, 25, 26] and cellular/tissue classification [27, 28, 29].

Since 2020 there has been a much greater volume of research published, most of which has involved the use of deep neural networks for automatic feature extraction and classification. Recent research has investigated a broader array of diagnostic outcomes, including the classification of primary cancer type [30, 59], mutation status [40, 52, 57], homologous recombination deficiency status [49], tumour-stroma reaction level [46], transcriptomic subtypes [33, 40], microsatellite instability [40], and epithelial-mesenchymal transition status [45]. Three additional prognostic outcomes have also been predicted in more recent literature - progression-free survival [37, 41, 56], relapse [52, 56], and treatment response [32, 33, 54, 55, 60].

Despite progress within a few specific outcomes, there was no obvious overall trend in the sizes of datasets used over time, either in terms of the number of slides or the number of participants. Similarly, there was no evidence that recent research included more rigorous internal validations, though external validations have been increasing in frequency - no research before 2021 included any external validation with ovarian cancer data, but seven studies published more recently did [39, 40, 42, 44, 51, 55, 58]. While these external validations were typically limited to small quantities of data, the inclusion of any external validation demonstrates progress from previous research. Such validations are essential to the clinical utility of these models as real-world implementation will require robustness to different sources of visual heterogeneity, with variation occurring across different data centres and within data centres over time. As this field continues to mature, we hope to see more studies conduct thorough validations with larger, high-quality independent datasets, including clearly reported protocols for patient recruitment and selection, pathology slide creation, and digitization. This will help to reduce the biases, limited reproducibility, and limited generalisability identified in most of the existing research in this domain.

### **Current Limitations and Future Recommendations**

A large proportion of published work did not provide sufficient clinical and pathological information to assess the risk of bias. It is important that AI researchers thoroughly report data provenance to understand the extent of heterogeneity in the dataset, and to understand whether this has been

appropriately accounted for in the study design. Modelling and analysis methods must also be thoroughly reported to improve reliability and reproducibility. Researchers may find it useful to refer to reporting checklists, such as *transparent reporting of a multivariable prediction model for individual prognosis or diagnosis* (TRIPOD) [71], to ensure that they have understood and reported all relevant details of their studies. In many studies, it is not clear how AI would fit in the clinical workflow, or whether there are limitations in how these methods could be applied. AI researchers should ensure they understand the clinical context of their data and potential models before undertaking research to reduce bias and increase utility. Ideally, this will involve regular interactions with expert clinicians, including histopathologists and oncologists.

To further improve reproducibility, we recommend that researchers should make code and data available where possible. It is relatively easy to publish code and generate documentation to enhance usability, and there are few drawbacks to doing so when publishing research. Making data available is more often difficult due to data security requirements and the potential storage costs, but it can provide benefits beyond the primary research of the original authors. Digital pathology research in ovarian cancer is currently limited by the lack of openly accessible data, leading to over-dependence on TCGA, and causing many researchers to painstakingly collate similar but distinct datasets. These datasets often contain little of the heterogeneity seen in multi-centre, multi-scanner data, making it difficult for researchers to train robust models or assess generalisability. Where heterogeneous data is included, it often includes small quantities of data which are different to the majority, introducing risks of bias and confounding rather than helping to overcome these issues. TCGA-based studies are prone to this, with significant differences between TCGA slides originating from different data centres [72], but with many of these centres only providing small quantities of data. Many researchers are reliant on open-access data, but there is a severe shortage of suitable open-access ovarian cancer histopathology data. Making such data available, with detailed protocols describing data creation, allows researchers to conduct more thorough analyses and significantly improve model generalisability and clinical implementability.

For AI to achieve clinical utility, it is essential that more robust validations are performed, especially considering the limitations of the available datasets. We recommend that researchers should always conduct thorough analyses, using cross-validation, bootstrapping, and/or external validations to ensure that results are robust and truly reflect the ability of their model(s) to generalise to unseen data, and are not simply caused by chance. This should include reporting the variability of results (typically in a 95% confidence interval), especially when comparing multiple models to help to distinguish whether one model is genuinely better than another or whether the difference is due to chance. Statistical tests can also be beneficial for these evaluations. Another option for capturing variability is Bayesian uncertainty quantification, which can be used to separate aleatoric (inherent) and epistemic (modelling) uncertainty.

Current literature in this field can be largely characterised as model prototyping with homogeneous retrospective data. Researchers rarely consider the reality of human-machine interaction, perhaps believing that these models are a drop-in replacement for pathologists. However, these models perform narrow tasks within the pathology pipeline and do not take into consideration the clinical context beyond their limited training datasets and siloed tasks. We believe these models would be more beneficial (and more realistic to implement) as assistive tools for pathologists, providing secondary opinions or novel ancillary information. While current research is typically focused on assessing model accuracy without any pathologist input, different study designs could be employed to better assess the real-world utility of these models as assistive tools. For example, usability studies could investigate which models are most accessible and most informative to pathologists in practice, and prospective studies could quantify any benefits to diagnostic efficiency and patient outcomes, and investigate the robustness of models in practice. Understanding the effects of AI on the efficiency of diagnosis is particularly important given the limited supply of pathologists worldwide. As such, this type of research will significantly benefit clinical translation.

## Summary of recommendations

- Understand data and ensure planned research is clinically relevant before modelling, ideally involving clinicians throughout the project.
- Consider different study designs, including usability studies and/or prospective studies.
- Clearly report the context of any histopathology data, including how patients were recruited/selected, and how tissue specimens were processed to generate digital pathology images.
- Conduct thorough analyses using cross-validation, external validation, and/or bootstrapping.
- Make all code openly accessible (and data if possible).

## ACKNOWLEDGMENTS

There was no direct funding for this research. JB is supported by the UKRI Engineering and Physical Sciences Research Council (EPSRC) [EP/S024336/1]. KA, PA are supported by the Tony Bramall Charitable Trust. AS is supported by Innovate UK via the National Consortium of Intelligent Medical Imaging (NCIMI) [104688], Cancer Research UK [C19942/A28832] and Leeds Hospitals Charity [9R01/1403]. The funders had no role in influencing the content of this research. For the purpose of open access, the author has applied a Creative Commons Attribution (CC BY) licence to any Author Accepted Manuscript version arising from this submission.

## AUTHOR CONTRIBUTIONS

JB created the study protocol with feedback and contributions from all other authors. JB, KA, KZ, NMO, and NR performed the risk of bias assessments. JB and KA performed data extraction. JB analysed extracted data and wrote the manuscript, with feedback and contributions from all other authors.

## COMPETING INTERESTS

GH receives research funding from IQVIA. NMO receives research funding from 4D Path. All other authors declare no conflicts of interest.

## REFERENCES

- [1] Hyuna Sung, Jacques Ferlay, Rebecca L. Siegel, Mathieu Laversanne, Isabelle Soerjomataram, Ahmedin Jemal, and Freddie Bray. Global cancer statistics 2020: Globocan estimates of incidence and mortality worldwide for 36 cancers in 185 countries. *CA: A Cancer Journal for Clinicians*, 71, 2021.
- [2] Usha Menon, Aleksandra Gentry-Maharaj, Matthew Burnell, Naveena Singh, Andy Ryan, Chloe Karpinskyj, Giulia Carlino, Julie Taylor, Susan K. Massingham, Maria Raikou, Jatinderpal K. Kalsi, Robert Woolas, Ranjit Manchanda, Rupali Arora, Laura Casey, Anne Dawnay, Stephen Dobbs, Simon Leeson, Tim Mould, Mourad W. Seif, Aarti Sharma, Karin Williamson, Yiling Liu, Lesley Fallowfield, Alistair J. McGuire, Stuart Campbell, Steven J. Skates, Ian J. Jacobs, and Mahesh Parmar. Ovarian cancer population screening and mortality after long-term follow-up in the uk collaborative trial of ovarian cancer screening (ukctocs): a randomised controlled trial. *The Lancet*, 397, 2021.
- [3] Mark H. Ebell, Marybeth B. Culp, and Taylor J. Radke. A systematic review of symptoms for the diagnosis of ovarian cancer. *American Journal of Preventive Medicine*, 50, 2016.
- [4] Jonathan S. Berek, Malte Renz, Sean Kehoe, Lalit Kumar, and Michael Friedlander. Cancer of the ovary, fallopian tube, and peritoneum: 2021 update. *International Journal of Gynecology and Obstetrics*, 155, 2021.
- [5] Martin Köbel, Steve E. Kalloger, Niki Boyd, Steven McKinney, Erika Mehl, Chana Palmer, Samuel Leung, Nathan J. Bowen, Diana N. Ionescu, Ashish Rajput, Leah M. Prentice, Dianne Miller, Jennifer Santos, Kenneth Swenerton, C. Blake Gilks, and David Huntsman. Ovarian



- carcinoma subtypes are different diseases: Implications for biomarker studies. *PLoS Medicine*, 5, 2008.
- [6] Jaime Prat. Staging classification for cancer of the ovary, fallopian tube, and peritoneum. *International Journal of Gynecology and Obstetrics*, 124:1–5, 2014.
- [7] Rayna K. Matsuno, Mark E. Sherman, Kala Visvanathan, Marc T. Goodman, Brenda Y. Hernandez, Charles F. Lynch, Olga B. Ioffe, David Horio, Charles Platz, Sean F. Altekruise, Ruth M. Pfeiffer, and William F. Anderson. Agreement for tumor grade of ovarian carcinoma: Analysis of archival tissues from the surveillance, epidemiology, and end results residual tissue repository. *Cancer Causes and Control*, 24, 2013.
- [8] Martin Köbel, Julia Bak, Björn I. Bertelsen, Olli Carpen, Anni Grove, Estrid S. Hansen, Anne Marie Levin Jakobsen, Marianne Lidang, Anna Måsbäck, Anna Tolf, C. Blake Gilks, and Joseph W. Carlson. Ovarian carcinoma histotype determination is highly reproducible, and is improved through the use of immunohistochemistry. *Histopathology*, 64, 2014.
- [9] Mollie E. Barnard, Alexander Pyden, Megan S. Rice, Miguel Linares, Shelley S. Tworoger, Brooke E. Howitt, Emily E. Meserve, and Jonathan L. Hecht. Inter-pathologist and pathology report agreement for ovarian tumor characteristics in the nurses' health studies. *Gynecologic Oncology*, 150, 2018.
- [10] Michael L. Wilson, Kenneth A. Fleming, Modupe A. Kuti, Lai Meng Looi, Nestor Lago, and Kun Ru. Access to pathology and laboratory medicine services: a crucial gap. *The Lancet*, 391, 2018.
- [11] Royal College of Pathologists. Meeting pathology demand: Histopathology workforce census. 2018.
- [12] Alexi Baidoshvili, Anca Bucur, Jasper van Leeuwen, Jeroen van der Laak, Philip Kluin, and Paul J. van Diest. Evaluating the benefits of digital pathology implementation: time savings in laboratory logistics. *Histopathology*, 73, 2018.
- [13] Albrecht Stenzinger, Maximilian Alber, Michael Allgäuer, Philipp Jurmeister, Michael Bockmayr, Jan Budczies, Jochen Lennerz, Johannes Eschrich, Daniel Kazdal, Peter Schirmacher, Alex H. Wagner, Frank Tacke, David Capper, Klaus Robert Müller, and Frederick Klauschen. Artificial intelligence and pathology: From principles to practice and future applications in histomorphology and molecular profiling. *Seminars in Cancer Biology*, 84, 2022.
- [14] Patricia Raciti, Jillian Sue, Juan A Retamero, Rodrigo Ceballos, Ran Godrich, Jeremy D Kunz, Adam Casson, Dilip Thiagarajan, Zahra Ebrahimzadeh, Julian Viret, et al. Clinical validation of artificial intelligence–augmented pathology diagnosis demonstrates significant gains in diagnostic accuracy in prostate cancer detection. *Archives of Pathology & Laboratory Medicine*, 2022.
- [15] Paula Dhiman, Jie Ma, Constanza L. Andaur Navarro, Benjamin Speich, Garrett Bullock, Johanna A. A. Damen, Lotty Hooft, Shona Kirtley, Richard D. Riley, Ben Van Galster, Karel G. M. Moons, and Gary S. Collins. Methodological conduct of prognostic prediction models developed using machine learning in oncology: a systematic review. *BMC Medical Research Methodology*, 22:101, 12 2022.
- [16] Robert F. Wolff, Karel G.M. Moons, Richard D. Riley, Penny F. Whiting, Marie Westwood, Gary S. Collins, Johannes B. Reitsma, Jos Kleijnen, and Sue Mallett. Probast: A tool to assess the risk of bias and applicability of prediction model studies. *Annals of Internal Medicine*, 170, 2019.
- [17] Jiwen Dong, Jing Li, Jian Lu, and Aifang Fu. Automatic segmentation for ovarian cancer immunohistochemical image based on chroma criterion. In *2010 2nd International Conference on Advanced Computer Control*, volume 2, pages 147–150. IEEE, 2010.
- [18] Jiwen Dong, Jing Li, Aifang Fu, and Huiming Lv. Automatic segmentation for ovarian cancer immunohistochemical image based on yuv color space. In *2010 International Conference on Biomedical Engineering and Computer Science*, pages 1–4. IEEE, 2010.
- [19] Nicolas Signolle, Marinette Revenu, Benoît Plancoulaine, and Paulette Herlin. Wavelet-based multiscale texture segmentation: Application to stromal compartment characterization on virtual slides. *Signal Processing*, 90, 2010.
- [20] Andrew Janowczyk, Sharat Chandran, Michael Feldman, and Anant Madabhushi. Local morphologic scale: application to segmenting tumor infiltrating lymphocytes in ovarian cancer tmas. In *Medical Imaging 2011: Image Processing*, volume 7962, pages 827–840. SPIE, 2011.

- [21] Andrew Janowczyk, Sharat Chandran, Rajendra Singh, Dimitra Sasaroli, George Coukos, Michael D. Feldman, and Anant Madabhushi. High-throughput biomarker segmentation on ovarian cancer tissue microarrays via hierarchical normalized cuts. *IEEE Transactions on Biomedical Engineering*, 59, 2012.
- [22] Sonal Kothari, John H Phan, Adeboye O Osunkoya, and May D Wang. Biological interpretation of morphological patterns in histopathological whole-slide images. In *Proceedings of the ACM conference on bioinformatics, computational biology and biomedicine*, pages 218–225, 2012.
- [23] Anjaly Poruthoor, John H Phan, Sonal Kothari, and May D Wang. Exploration of genomic, proteomic, and histopathological image data integration methods for clinical prediction. In *2013 IEEE China Summit and International Conference on Signal and Information Processing*, pages 259–263. IEEE, 2013.
- [24] Aicha BenTaieb, Hector Li-Chang, David Huntsman, and Ghassan Hamarneh. Automatic diagnosis of ovarian carcinomas via sparse multiresolution tissue representation. In *Medical Image Computing and Computer-Assisted Intervention—MICCAI 2015: 18th International Conference, Munich, Germany, October 5-9, 2015, Proceedings, Part I 18*, pages 629–636. Springer, 2015.
- [25] Aicha BenTaieb, Masoud S Nosrati, Hector Li-Chang, David Huntsman, and Ghassan Hamarneh. Clinically-inspired automatic classification of ovarian carcinoma subtypes. *Journal of pathology informatics*, 7(1):28, 2016.
- [26] Aicha BenTaieb, Hector Li-Chang, David Huntsman, and Ghassan Hamarneh. A structured latent model for ovarian carcinoma subtyping from histopathology slides. *Medical image analysis*, 39:194–205, 2017.
- [27] Auranuch Lorsakul, Emilia Andersson, Suzana Vega Haring, Hadassah Sade, Oliver Grimm, and Joerg Bredno. Automated wholeslide analysis of multiplex-brightfield ihc images for cancer cells and carcinoma-associated fibroblasts. In *Medical Imaging 2017: Digital Pathology*, volume 10140, pages 41–46. SPIE, 2017.
- [28] Yue Du, Roy Zhang, Abolfazl Zargari, Theresa C. Thai, Camille C. Gunderson, Katherine M. Moxley, Hong Liu, Bin Zheng, and Yuchen Qiu. Classification of tumor epithelium and stroma by exploiting image features learned by deep convolutional neural networks. *Annals of Biomedical Engineering*, 46, 2018.
- [29] Andreas Heindl, Adnan Mujahid Khan, Daniel Nava Rodrigues, Katherine Eason, Anguraj Sadanandam, Cecilia Orbegoso, Marco Punta, Andrea Sottoriva, Stefano Lise, Susana Banerjee, and Yinyin Yuan. Microenvironmental niche divergence shapes brca1-dysregulated ovarian cancer morphological plasticity. *Nature Communications*, 9, 2018.
- [30] Shivam Kalra, H. R. Tizhoosh, Sultaan Shah, Charles Choi, Savvas Damaskinos, Amir Safarpour, Sobhan Shafiei, Morteza Babaie, Phedias Diamandis, Clinton J.V. Campbell, and Liron Pantanowitz. Pan-cancer diagnostic consensus through searching archival histopathology images using artificial intelligence. *npj Digital Medicine*, 3, 2020.
- [31] Adrian B. Levine, Jason Peng, David Farnell, Mitchell Nursey, Yiping Wang, Julia R. Naso, Hezhen Ren, Hossein Farahani, Colin Chen, Derek Chiu, Aline Talhouk, Brandon Sheffield, Maziar Riazzy, Philip P. Ip, Carlos Parra-Herran, Anne Mills, Naveena Singh, Basile Tessier-Cloutier, Taylor Salisbury, Jonathan Lee, Tim Salcudean, Steven J.M. Jones, David G. Huntsman, C. Blake Gilks, Stephen Yip, and Ali Bashashati. Synthesis of diagnostic quality cancer pathology images by generative adversarial networks. *Journal of Pathology*, 252, 2020.
- [32] Asfand Yaar, Amina Asif, Shan E Ahmed Raza, Nasir Rajpoot, and Fayyaz Minhas. Cross-domain knowledge transfer for prediction of chemosensitivity in ovarian cancer patients. In *Proceedings of the IEEE/CVF Conference on Computer Vision and Pattern Recognition Workshops*, pages 928–929, 2020.
- [33] Kun Hsing Yu, Vincent Hu, Feiran Wang, Ursula A. Matulonis, George L. Mutter, Jeffrey A. Golden, and Isaac S. Kohane. Deciphering serous ovarian carcinoma histopathology and platinum response by convolutional neural networks. *BMC Medicine*, 18, 2020.
- [34] Lucy Gentles, Rachel Howarth, Won Ji Lee, Sweta Sharma-Saha, Angela Ralte, Nicola Curtin, Yvette Drew, and Rachel Louise O'Donnell. Integration of computer-aided automated analysis algorithms in the development and validation of immunohistochemistry biomarkers in ovarian cancer. *Journal of Clinical Pathology*, 74, 2021.

- [35] Rania M. Ghoniem, Abeer D. Algarni, Basel Refky, and Ahmed A. Ewees. Multi-modal evolutionary deep learning model for ovarian cancer diagnosis. *Symmetry*, 13, 2021.
- [36] Jun Jiang, Burak Tekin, Ruifeng Guo, Hongfang Liu, Yajue Huang, and Chen Wang. Digital pathology-based study of cell- and tissue-level morphologic features in serous borderline ovarian tumor and high-grade serous ovarian cancer. *Journal of Pathology Informatics*, 12, 2021.
- [37] Anna Ray Laury, Sami Blom, Tuomas Ropponen, Anni Virtanen, and Olli Mikael Carpén. Artificial intelligence-based image analysis can predict outcome in high-grade serous carcinoma via histology alone. *Scientific Reports*, 11, 2021.
- [38] S. T. Paijens, A. Vledder, D. Loiero, E. W. Duiker, J. Bart, A. M. Hendriks, M. Jalving, H. H. Workel, H. Hollema, N. Werner, A. Plat, G. B.A. Wisman, R. Yigit, H. Arts, A. J. Kruse, N. M. de Lange, V. H. Koelzer, M. de Bruyn, and H. W. Nijman. Prognostic image-based quantification of cd8cd103 t cell subsets in high-grade serous ovarian cancer patients. *OncolImmunology*, 10, 2021.
- [39] Seo Jeong Shin, Seng Chan You, Hokyun Jeon, Ji Won Jung, Min Ho An, Rae Woong Park, and Jin Roh. Style transfer strategy for developing a generalizable deep learning application in digital pathology. *Computer Methods and Programs in Biomedicine*, 198:105815, 2021.
- [40] Hao Zeng, Linyan Chen, Mingxuan Zhang, Yuling Luo, and Xuelei Ma. Integration of histopathological images and multi-dimensional omics analyses predicts molecular features and prognosis in high-grade serous ovarian cancer. *Gynecologic Oncology*, 163, 2021.
- [41] Kevin M. Boehm, Emily A. Aherne, Lora Ellenson, Ines Nikolovski, Mohammed Alghamdi, Ignacio Vázquez-García, Dmitriy Zamarin, Kara Long Roche, Ying Liu, Druv Patel, Andrew Aukerman, Arfath Pasha, Doori Rose, Pier Selenica, Pamela I. Causa Andrieu, Chris Fong, Marinela Capanu, Jorge S. Reis-Filho, Rami Vanguri, Harini Veeraraghavan, Natalie Gangai, Ramon Sosa, Samantha Leung, Andrew McPherson, Jian Jiong Gao, Yulia Lakhman, and Sohrab P. Shah. Multimodal data integration using machine learning improves risk stratification of high-grade serous ovarian cancer. *Nature Cancer*, 3:723–733, 6 2022.
- [42] Jeffrey Boschman, Hossein Farahani, Amirali Darbandsari, Pouya Ahmadvand, Ashley Van Spankeren, David Farnell, Adrian B. Levine, Julia R. Naso, Andrew Churg, Steven J.M. Jones, Stephen Yip, Martin Köbel, David G. Huntsman, C. Blake Gilks, and Ali Bashashati. The utility of color normalization for ai-based diagnosis of hematoxylin and eosin-stained pathology images. *Journal of Pathology*, 256, 2022.
- [43] Nicolas Elie, Florence Giffard, Cécile Blanc-Fournier, Pierre Marie Morice, Pierre Emmanuel Brachet, Soizic Dutoit, Benoît Plancoulaine, and Laurent Poulain. Impact of automated methods for quantitative evaluation of immunostaining: Towards digital pathology. *Frontiers in Oncology*, 12, 10 2022.
- [44] Hossein Farahani, Jeffrey Boschman, David Farnell, Amirali Darbandsari, Allen Zhang, Pouya Ahmadvand, Steven J. M. Jones, David Huntsman, Martin Köbel, C. Blake Gilks, Naveena Singh, and Ali Bashashati. Deep learning-based histotype diagnosis of ovarian carcinoma whole-slide pathology images. *Modern Pathology*, 35:1983–1990, 12 2022.
- [45] Yang Hu, Korsuk Sirinukunwattana, Kezia Gaitskell, Ruby Wood, Clare Verrill, and Jens Rittscher. Predicting molecular traits from tissue morphology through self-interactive multi-instance learning. In *Medical Image Computing and Computer Assisted Intervention—MICCAI 2022: 25th International Conference, Singapore, September 18–22, 2022, Proceedings, Part II*, pages 130–139. Springer, 2022.
- [46] Jun Jiang, Burak Tekin, Lin Yuan, Sebastian Armasu, Stacey J. Winham, Ellen L. Goode, Hongfang Liu, Yajue Huang, Ruifeng Guo, and Chen Wang. Computational tumor stroma reaction evaluation led to novel prognosis-associated fibrosis and molecular signature discoveries in high-grade serous ovarian carcinoma. *Frontiers in Medicine*, 9, 9 2022.
- [47] Kokila R. Kasture, Dharmaveer Choudhari, and Pravin N. Matte. Prediction and classification of ovarian cancer using enhanced deep convolutional neural network. *International Journal of Engineering Trends and Technology*, 70:310–318, 3 2022.
- [48] Piotr A Kowalski, Jakub Błoniarczyk, and Łukasz Chmura. Convolutional neural networks in the ovarian cancer detection. In *Computational Intelligence and Mathematics for Tackling Complex Problems 2*, pages 55–64. Springer, 2022.

- [49] Tristan Lazard, Guillaume Bataillon, Peter Naylor, Tatiana Popova, François-Clément Bidard, Dominique Stoppa-Lyonnet, Marc-Henri Stern, Etienne Decencière, Thomas Walter, and Anne Vincent-Salomon. Deep learning identifies morphological patterns of homologous recombination deficiency in luminal breast cancers from whole slide images. *Cell Reports Medicine*, 3(12):100872, 2022.
- [50] Tianling Liu, Ran Su, Changming Sun, Xiuting Li, and Leyi Wei. Eocsa: Predicting prognosis of epithelial ovarian cancer with whole slide histopathological images. *Expert Systems with Applications*, 206, 11 2022.
- [51] Robin S Mayer, Steffen Gretser, Lara E Heckmann, Paul K Ziegler, Britta Walter, Henning Reis, Katrin Bankov, Sven Becker, Jochen Triesch, Peter J Wild, et al. How to learn with intentional mistakes: Noisyensembles to overcome poor tissue quality for deep learning in computational pathology. *Frontiers in Medicine*, 9, 2022.
- [52] Camilla Nero, Luca Boldrini, Jacopo Lenkiewicz, Maria Teresa Giudice, Alessia Piermattei, Frediano Inzani, Tina Pasciuto, Angelo Minucci, Anna Fagotti, Gianfranco Zannoni, Vincenzo Valentini, and Giovanni Scambia. Deep-learning to predict brca mutation and survival from digital h&e slides of epithelial ovarian cancer. *International Journal of Molecular Sciences*, 23, 10 2022.
- [53] Jennifer Salguero, Prateek Prasanna, Germán Corredor, Angel Cruz-Roa, David Becerra, and Eduardo Romero. Selecting training samples for ovarian cancer classification via a semi-supervised clustering approach. In *Medical Imaging 2022: Digital and Computational Pathology*, volume 12039, pages 20–24. SPIE, 2022.
- [54] Ching-Wei Wang, Yu-Ching Lee, Cheng-Chang Chang, Yi-Jia Lin, Yi-An Liou, Po-Chao Hsu, Chun-Chieh Chang, Aung-Kyaw-Oo Sai, Chih-Hung Wang, and Tai-Kuang Chao. A weakly supervised deep learning method for guiding ovarian cancer treatment and identifying an effective biomarker. *Cancers*, 14(7):1651, 2022(a).
- [55] Ching Wei Wang, Cheng Chang Chang, Yu Ching Lee, Yi Jia Lin, Shih Chang Lo, Po Chao Hsu, Yi An Liou, Chih Hung Wang, and Tai Kuang Chao. Weakly supervised deep learning for prediction of treatment effectiveness on ovarian cancer from histopathology images. *Computerized Medical Imaging and Graphics*, 99, 7 2022(b).
- [56] Ryo Yokomizo, Tiago JS Lopes, Nagisa Takashima, Sou Hirose, Ayako Kawabata, Masataka Takenaka, Yasushi Iida, Nozomu Yanaiharu, Kei Yura, Haruhiko Sago, et al. O3c glass-class: A machine-learning framework for prognostic prediction of ovarian clear-cell carcinoma. *Bioinformatics and Biology Insights*, 16:11779322221134312, 2022.
- [57] David Joon Ho, M Herman Chui, Chad M Vanderbilt, Jiwon Jung, Mark E Robson, Chan-Sik Park, Jin Roh, and Thomas J Fuchs. Deep interactive learning-based ovarian cancer segmentation of h&e-stained whole slide images to study morphological patterns of brca mutation. *Journal of Pathology Informatics*, 14:100160, 2023.
- [58] Zhu Meng, Guangxi Wang, Fei Su, Yan Liu, Yuxiang Wang, Jing Yang, Jianyuan Luo, Fang Cao, Panpan Zhen, Binhua Huang, et al. A deep learning-based system trained for gastrointestinal stromal tumor screening can identify multiple types of soft tissue tumors. *The American Journal of Pathology*, 2023.
- [59] Sathya Ramasamy and Vaidehi Kaliyaperumal. A hybridized channel selection approach with deep convolutional neural network for effective ovarian cancer prediction in periodic acid-schiff-stained images. *Concurrency and Computation: Practice and Experience*, 35(5):e7568, 2023.
- [60] Ching-Wei Wang, Yu-Ching Lee, Yi-Jia Lin, Chun-Chieh Chang, Chih-Hung Wang, Tai-Kuang Chao, et al. Interpretable attention-based deep learning ensemble for personalized ovarian cancer treatment without manual annotations. *Computerized Medical Imaging and Graphics*, 107:102233, 2023.
- [61] Meixuan Wu, Chengguang Zhu, Jiani Yang, Shanshan Cheng, Xiaokang Yang, Sijia Gu, Shilin Xu, Yongsong Wu, Wei Shen, Shan Huang, et al. Exploring prognostic indicators in the pathological images of ovarian cancer based on a deep survival network. *Frontiers in Genetics*, 13, 2023.
- [62] Chandra Holback, Rose Jarosz, Fred Prior, David G Mutch, Priya Bhosale, Kimberly Garcia, Yueh Lee, Shanah Kirk, Cheryl A Sadow, Seth Levine, Evis Sala, Pierre Elnajjar, Tara Morgan,

- and Brad Erickson. The cancer genome atlas ovarian cancer collection (tcga-ov) (version 4) [data set]. *The Cancer Imaging Archive*, 2016.
- [63] Martin Köbel, Steve E. Kalloger, Patricia M. Baker, Carol A. Ewanowich, Jocelyne Arseneau, Viktor Zhrebetskiy, Soran Abdulkarim, Samuel Leung, Máire A. Duggan, Dan Fontaine, Robin Parker, David G. Huntsman, and C. Blake Gilks. Diagnosis of ovarian carcinoma cell type is highly reproducible: A transcanadian study. *American Journal of Surgical Pathology*, 34, 2010.
- [64] Maximilian Ilse, Jakub Tomczak, and Max Welling. Attention-based deep multiple instance learning. In *International conference on machine learning*, pages 2127–2136. PMLR, 2018.
- [65] Ming Y. Lu, Drew F.K. Williamson, Tiffany Y. Chen, Richard J. Chen, Matteo Barbieri, and Faisal Mahmood. Data-efficient and weakly supervised computational pathology on whole-slide images. *Nature Biomedical Engineering*, 5, 2021.
- [66] Kelei He, Chen Gan, Zhuoyuan Li, Islem Rekik, Zihao Yin, Wen Ji, Yang Gao, Qian Wang, Junfeng Zhang, and Dinggang Shen. Transformers in medical image analysis: A review. *Intelligent Medicine*, 2022.
- [67] Pallabi Shrestha, Bhavya Poudyal, Sepideh Yadollahi, Darryl E Wright, Adriana V Gregory, Joshua D Warner, Panagiotis Korfiatis, Isabel C Green, Sarah L Rassier, Andrea Mariani, et al. A systematic review on the use of artificial intelligence in gynecologic imaging—background, state of the art, and future directions. *Gynecologic Oncology*, 2022.
- [68] Jingyang Zhou, Weiwei Cao, Lan Wang, Zezheng Pan, and Ying Fu. Application of artificial intelligence in the diagnosis and prognostic prediction of ovarian cancer. *Computers in Biology and Medicine*, page 105608, 2022.
- [69] Oraianthi Fiste, Michalis Liontos, Flora Zagouri, Georgios Stamatakos, and Meletios Athanasios Dimopoulos. Machine learning applications in gynecological cancer: a critical review. *Critical Reviews in Oncology/Hematology*, page 103808, 2022.
- [70] He-Li Xu, Ting-Ting Gong, Fang-Hua Liu, Hong-Yu Chen, Qian Xiao, Yang Hou, Ying Huang, Hong-Zan Sun, Yu Shi, Song Gao, et al. Artificial intelligence performance in image-based ovarian cancer identification: A systematic review and meta-analysis. *EClinicalMedicine*, 53:101662, 2022.
- [71] Gary S Collins, Johannes B Reitsma, Douglas G Altman, and Karel GM Moons. Transparent reporting of a multivariable prediction model for individual prognosis or diagnosis (tripod): the tripod statement. *Annals of internal medicine*, 162(1):55–63, 2015.
- [72] Taher Dehkharghanian, Azam Asilian Bidgoli, Abtin Riasatian, Pooria Mazaheri, Clinton JV Campbell, Liron Pantanowitz, HR Tizhoosh, and Shahryar Rahnamayan. Biased data, biased ai: deep networks predict the acquisition site of tcga images. *Diagnostic Pathology*, 18(1):1–12, 2023.

## A SEARCH STRATEGY

Searches for all databases are shown here, with any text which is not directly input to the search bar in **bold** font. These searches are each a combination of three aspects - artificial intelligence, ovarian cancer, and histopathology. No filters were applied, and all options were left on their default settings. The wildcard character, \*, was used to search for multiple versions of the same word, for example, "patholog\*" searches for all of "pathology", "pathologist", "pathologists", and "pathological".

### A.1 PubMed

("Machine Learning"[Mesh] OR "Artificial Intelligence"[Mesh] OR "Neural Networks, Computer"[Mesh] OR "support vector machine"[MeSH] OR "Deep Learning"[Mesh] OR "diagnosis, computer-assisted"[Mesh] OR "Machine learn\*" OR "Artificial Intelligen\*" OR (ML[Title/Abstract] NOT ( $\mu$ gml[Title/Abstract] OR  $\mu$ /ml[Title/Abstract] OR mgml[Title/Abstract] OR pgml[Title/Abstract] OR ngml[Title/Abstract] OR uiml[Title/Abstract] OR iuml[Title/Abstract] OR miuml[Title/Abstract] OR muiml[Title/Abstract] OR uml[Title/Abstract] OR gml[Title/Abstract] OR mlkg[Title/Abstract] OR milliliter\*[Title/Abstract])) OR AI[Title/Abstract] OR "Computer Vision" OR "Neural network\*" OR "Deep Network\*" OR "Computer-aided Diagnosis" OR "Computer aided Diagnosis" OR Perceptron\* OR "Convolutional Network\*" OR "Recurrent Network\*" OR "Graph Network\*" OR "Deep Learn\*" OR "Deep-Learn\*" OR Backprop\* OR "support vector\*" OR ensemble\* OR "random forest\*" OR "nearest neighbor\*" OR "nearest neighbour\*" OR "k-nearest neighbor\*" OR "k-nearest neighbour\*" OR "Gradient boost\*" OR "XGBoost\*" OR "segmentation" OR "instance learning" OR "multi-instance learning" OR "Active Learning")

AND (((ovar\* OR fallopian) AND (cancer\* OR mass\* OR carcinoma\* OR tumour\* OR tumor\* OR neoplasm\* OR malignan\* OR "carcinoma"[Mesh] OR "neoplasms"[Mesh])) OR "Ovarian Neoplasms"[Mesh] OR "peritoneal cancer" OR "peritoneal carcinoma" OR "peritoneal tumo\*")

AND ((digit\* AND patholog\*) OR "computational patholog\*" OR "tissue microarray\*" OR histopath\* OR histolog\* OR "Whole Slide Imag\*" OR "Tissue slide\*" OR "pathology slide\*" OR "pathology image\*" OR Immunohistochem\* OR ((Haematoxylin OR Hematoxylin) AND Eosin) OR Histology[Mesh])

### A.2 Scopus

TITLE-ABS-KEY("Machine learn\*" OR "Artificial Intelligen\*" OR ("ML" AND NOT "\*  $\mu$  ml" AND NOT "\*g ml" AND NOT "\*ui ml" AND NOT "\*UI ml" AND NOT "\*iu ml" AND NOT "\*u ml" AND NOT "\*g ml" AND NOT "\*ml kg" AND NOT milliliter\*)) OR AI OR "Computer Vision" OR "Neural network\*" OR "Deep Network\*" OR "Computer-aided Diagnosis" OR "Computer aided Diagnosis" OR Perceptron\* OR "Convolutional Network\*" OR "Recurrent Network\*" OR "Graph Network\*" OR "Deep Learn\*" OR "Deep-Learn\*" OR Backprop\* OR "support vector\*" OR ensemble\* OR "random forest\*" OR "nearest neighbor\*" OR "nearest neighbour\*" OR "k-nearest neighbor\*" OR "k-nearest neighbour\*" OR "Gradient boost\*" OR "XGBoost\*" OR "segmentation" OR "instance learning" OR "multi-instance learning" OR "Active Learning")

AND TITLE-ABS-KEY(((ovar\* OR fallopian) AND (cancer\* OR mass\* OR carcinoma\* OR tumour\* OR tumor\* OR neoplasm\* OR malignan\*)) OR "peritoneal cancer" OR "peritoneal carcinoma" OR "peritoneal tumo\*")

AND TITLE-ABS-KEY((digit\* AND patholog\*) OR "computational patholog\*" OR "tissue microarray\*" OR histopath\* OR histolog\* OR "Whole Slide Imag\*" OR "Tissue slide\*" OR "pathology slide\*" OR "pathology image\*" OR Immunohistochem\* OR ((Haematoxylin OR Hematoxylin) AND Eosin))

### A.3 Web of Science

(ALL=("Machine learn\*" OR "Artificial Intelligen\*" OR "Computer Vision" OR "Neural network\*" OR "Deep Network\*" OR "Computer-aided Diagnosis" OR "Computer aided Diagnosis" OR Perceptron\* OR "Convolutional Network\*" OR "Recurrent Network\*" OR "Graph Network\*" OR "Deep Learn\*" OR "Deep-Learn\*" OR Backprop\* OR "support vector\*" OR ensemble\* OR "random forest\*" OR "nearest neighbor\*" OR "nearest neighbour\*" OR "k-nearest neighbor\*" OR "k-nearest neighbour\*" OR "Gradient boost\*" OR "XGBoost\*" OR "segmentation" OR "instance learning" OR "multi-instance learning" OR "Active Learning") OR TS=(AI OR ("ML" NOT ("\*  $\mu$  ml" OR "\*g ml" OR "\*ui ml" OR "\*UI ml" OR "\*iu ml" OR "\*u ml" OR "\*g ml" OR "\*ml kg" OR milliliter\*))))

AND ALL=(((ovar\* OR fallopian) AND (cancer\* OR mass\* OR carcinoma\* OR tumour\* OR tumor\* OR neoplasm\* OR malignan\*)) OR "peritoneal cancer" OR "peritoneal carcinoma" OR "peritoneal tumo\*")

AND ALL=((digit\* AND patholog\*) OR "computational patholog\*" OR "tissue microarray\*" OR histopath\* OR histolog\* OR "Whole Slide Imag\*" OR "Tissue slide\*" OR "pathology slide\*" OR "pathology image\*" OR Immunohistochem\* OR ((Haematoxylin OR Hematoxylin) AND Eosin))

#### **A.4 Cochrane Central Register of Controlled Trials**

##### **Search #1:**

**All text:** ("Machine learn\*" OR "Artificial Intelligen\*" OR "Computer Vision" OR "Neural network\*" OR "Deep Network\*" OR "Computer-aided Diagnosis" OR "Computer aided Diagnosis" OR Perceptron\* OR "Convolutional Network\*" OR "Recurrent Network\*" OR "Graph Network\*" OR "Deep Learn\*" OR "Deep-Learn\*" OR Backprop\* OR "support vector\*" OR ensemble\* OR "random forest\*" OR "nearest neighbor\*" OR "nearest neighbour\*" OR "k-nearest neighbor\*" OR "k-nearest neighbour\*" OR "Gradient boost\*" OR "XGBoost\*" OR "segmentation" OR "instance learning" OR "multi-instance learning" OR "Active Learning")

##### **Search #2:**

**Title-Abstract-Keyword:** ("AI" OR ("ML" NOT ("\* μ ml" OR "\*g ml" OR "\*ui ml" OR "\*UI ml" OR "\*iu ml" OR "\*u ml" OR "\*g ml" OR "\*ml kg" OR milliliter\*))) in Title Abstract Keyword

##### **Search #3:**

**All text:** (((ovar\* OR fallopian) AND (cancer\* OR mass\* OR carcinoma\* OR tumour\* OR tumor\* OR neoplasm\* OR malignan\*)) OR "peritoneal cancer" OR "peritoneal carcinoma" OR "peritoneal tumo\*")

AND ((digit\* AND patholog\*) OR "computational patholog\*" OR "tissue microarray\*" OR histopath\* OR histolog\* OR "Whole Slide Imag\*" OR "Tissue slide\*" OR "pathology slide\*" OR "pathology image\*" OR Immunohistochem\* OR ((Haematoxylin OR Hematoxylin) AND Eosin))

##### **Final search:**

(#1 OR #2) AND #3

#### **A.5 WHO-ICTRP**

((("Machine learn\*" OR "Artificial Intelligen\*" OR "Computer Vision" OR "Neural network\*" OR "Deep Network\*" OR "Computer-aided Diagnosis" OR "Computer aided Diagnosis" OR Perceptron\* OR "Convolutional Network\*" OR "Recurrent Network\*" OR "Graph Network\*" OR "Deep Learn\*" OR "Deep-Learn\*" OR Backprop\* OR "support vector\*" OR ensemble\* OR "random forest\*" OR "nearest neighbor\*" OR "nearest neighbour\*" OR "k-nearest neighbor\*" OR "k-nearest neighbour\*" OR "Gradient boost\*" OR "XGBoost\*" OR "segmentation" OR "instance learning" OR "multi-instance learning" OR "Active Learning") OR ("AI" OR ("ML" NOT ("μ/ml" OR "g/ml" OR "ui/ml" OR "UI/ml" OR "iu/ml" OR "u/ml" OR "g/ml" OR "ml/kg" OR milliliter\*))))

AND (((ovar\* OR fallopian) AND (cancer\* OR mass\* OR carcinoma\* OR tumour\* OR tumor\* OR neoplasm\* OR malignan\*)) OR "peritoneal cancer" OR "peritoneal carcinoma" OR "peritoneal tumo\*")

AND ((digit\* AND patholog\*) OR "computational patholog\*" OR "tissue microarray\*" OR histopath\* OR histolog\* OR "Whole Slide Imag\*" OR "Tissue slide\*" OR "pathology slide\*" OR "pathology image\*" OR Immunohistochem\* OR ((Haematoxylin OR Hematoxylin) AND Eosin))

## B DATA EXTRACTION

Category	Fields
Overview	Internal ID. Lead author. Year. Conference/Journal name.
Data	Number of development images. Total number of images. Type of samples. FFPE/Frozen. Size of images. Tissue of origin. Number of development patients. Total number of patients. Number of data collection centres. Type of stain. Number of stainers. Scanners. Number of scanner types. Number of tissue processing centres. Data origin countries. Number of pathologists for data labelling. Online dataset. Prospective/retrospective. Clinical/research tissue. Data annotation. Maximum magnification available. Supplementary datatypes. Data exclusion reasons. Number of images excluded. Other cancer types included.
Methods	Outcome. Outcome measure/classes. Outcome standards/definition. Magnifications used. Patch sizes. Patches per image. Task type. Feature extraction type. Feature extractors. AI in main method. Other AI methods. Optimiser. Number of external validations. Differences to external validation set. Total external validation images. Number of cross-validation folds. Number of non-novel methods compared. Number of GPUs. Type of GPUs.
Results	Internal test accuracy, error bounds. AUC, error bounds. Sensitivity/specificity, error bounds. Other metric 1, error bounds. Other metric 2, error bounds. Other metric 3, error bounds. External training type. External test accuracy, error bounds. AUC, error bounds. Sensitivity/specificity, error bounds. Other metric 1, error bounds. Other metric 2, error bounds. Other metric 3, error bounds. Type of error bounds. Model training time. Visualisation type.
Miscellaneous	Code availability. Data availability. Notes

**Table 4.** Summary of the fields used for data extraction. The full form is available at [www.github.com/scjbb/OvCaReview](http://www.github.com/scjbb/OvCaReview).